Continental Shelf Research
August 2018, Volume 165 Pages 106-119
https://doi.org/10.1016/j.csr.2018.06.010
https://archimer.ifremer.fr/doc/00445/55628/

Constraining the origin of recently deposited particles using natural radionuclides ^{7}Be and $^{234}Th_{ex}$ in deltaic sediments

Wu Junwen [1, 2, 3, 5], Rabouille Christophe [2, 3, *], Charmasson Sabine [1, *], Reyss Jean Louis [2, 3], Cagnat Xavier [4]

[1] Ctr IFREMER Mediterranee, IRSN, PSE ENV SRTE Lab Rech Transferts Radionucleides S, CS 20330,Zone Portuaire Bregaillon, F-83507 La Seyne Sur Mer, France.
[2] UMR CEA CNRS UVSQ, LSCE, Ave Terrasse, F-91190 Gif Sur Yvette, France.
[3] IPSL, Ave Terrasse, F-91190 Gif Sur Yvette, France.
[4] IRSN, PSE ENV STEME, LMRE, F-91400 Orsay, France.
[5] Shantou Univ, Coll Sci, Shantou 515063, Peoples R China.

* Corresponding authors : Christophe Rabouille, email address : christophe.rabouille@lsce.ipsl.fr ; Sabine Charmasson, email address : sabine.charmasson@irsn.fr

Abstract :

^{7}Be and $^{234}Th_{ex}$ activities were determined in sediment cores off the Rhône River mouth (Gulf of Lions), in order to trace the initial transport and deposition of riverine suspended particulate matter (SPM) and evaluate the impact of flood events through 7 cruises carried out between 2007 and 2008. Consistently high ^{7}Be and $^{234}Th_{ex}$ inventories of 2000–3000 mBq cm^{-2} and 3000–5000 mBq cm^{-2}, respectively, were observed within a ~5 km radius off the Rhône River mouth. Their spatial distributions showed a gradual decrease with increasing distance from the Rhône River mouth, and the decrease in ^{7}Be was more pronounced than that of $^{234}Th_{ex}$, indicating that recent riverine SPM is rapidly deposited in the area located near the river mouth. This area is also characterized by high accumulation rates determined using ^{137}Cs or $^{210}Pb_{ex}$. Both ^{7}Be and $^{234}Th_{ex}$ inventories increased in 2008 compared to 2007, and are correlated to the cumulated SPM flux for normal and flood discharge. Moreover, the $^{7}Be/^{234}Th_{ex}$ inventory ratio appears to be a potential tracer to identify the dominant influence of recently deposited particles between terrestrial and marine waters. This ratio provides an effective tool to assess river and marine influence: Zone I at a distance inferior to 3.0 km, with $^{7}Be/^{234}Th_{ex}$ inventory ratio over 0.50 (surface area near river mouth ~ 7 km^2) is dominated by riverine influence; in contrast, Zone III at a distance superior to 8.5 km, with $^{7}Be/^{234}Th_{ex}$ inventory ratio less than 0.10 (surface area off river mouth beyond 150 km^2) is predominantly under a marine influence. In between, an intermediate area (Zone II at a distance between 3.0 and 8.5 km, with $^{7}Be/^{234}Th_{ex}$ inventory ratios between 0.10 and 0.50) displays a mixed influence. This zoning could help in further understanding the spreading of particle-reactive contaminants and its initial sedimentary deposition in the Gulf of Lions.

Highlights

► Short-term deposition of particles near the Rhône mouth was traced by ^{7}Be and $^{234}Th_{ex}$. ► Both ^{7}Be and $^{234}Th_{ex}$ inventories were correlated with the cumulated particle fluxes. ► Recent riverine particles are mainly deposited within 5 km off the Rhône river mouth. ► $^{7}Be/^{234}Th_{ex}$ inventory ratio was used to assess riverine and marine influence.

Keywords : ^{7}Be, ^{234}Th, Suspended particulate matter, Rhone River, 2008 flood, Gulf of Lions

1. Introduction

River-dominated ocean margins are among the most biogeochemically dynamic regions of the world and play a dominant role in global biogeochemical cycles (Dagg et al., 2004; McKee et al., 2004; Cai, 2011). These areas are highly efficient filters and transformers of terrestrial materials, and are key interfaces between the continent and the open ocean (Bianchi and Allison, 2009; Chen and Borges, 2009). Most of the river suspended particulate matter (SPM) is deposited in continental margin areas and less than 5% reach the deep sea (McKee et al., 2004). The SPM undergoes a series of processes associated with deposition and resuspension cycles after its initial discharge under different hydrological conditions (Sanford, 1992), especially during river floods and ocean storms. Consequently, the study of SPM deposition in the coastal zone under different hydrological regimes, such as short-term flood events, would help in understanding the fate of terrigenous pollutants carried by the SPM in river-dominated ocean margins.

Natural and artificial radionuclides have been widely used to investigate various processes in estuarine, coastal and marine environments (e.g., Santschi et al., 1999; Yeager et al., 2004; Moore and Oliveira, 2008; Su et al., 2011). Generally, flood events occur over very short time-scales (from days to weeks). Therefore, radionuclides with short half-lives, such as ^{7}Be ($t_{1/2}$=53.3 days) and ^{234}Th ($t_{1/2}$=24.1 days), appear to be appropriate tracers for studying flood deposition processes over these short time scales (Feng et al., 1999a; Saari et al., 2010). Resuspension may play a role in redistributing the original deposition and may mix sediments of different origins and age (Ogston et al., 2008).

Beryllium-7 (^{7}Be) is produced by cosmic ray spallation of nitrogen and oxygen in the atmosphere. ^{7}Be is a particle-reactive element and its distribution coefficient (K_d, L/kg) is estimated to be ~10^5 in estuarine and coastal waters (Dibb and Rice, 1989; Baskaran and Swarzenski, 2007). Following its formation in the stratosphere and troposphere, ^{7}Be is scavenged by submicron aerosol particles and is delivered to land principally through precipitation and dry deposition (Lal et al., 1958; Wallbrink and Murray, 1994) and then to rivers through watershed washout (Matisoff et al., 2002). ^{7}Be is generally used to study various processes over short time-scales, such as soil redistribution and erosion rates,

sediment residence time and transport in coastal and estuarine systems (Dibb and Rice, 1989; Sommerfield et al., 1999; Taylor et al., 2013). Another highly particle-reactive element, Thorium-234 (^{234}Th), with K_d up to ~10^5-10^6 (Guo et al., 1995; IAEA, 2004; Baskaran and Swarzenski, 2007), is produced from the decay of dissolved ^{238}U and is commonly present in excess (ex) of its parent ^{238}U in coastal suspended matter and bottom sediments (Aller and Cochran, 1976). ^{238}U concentrations in rivers and oceans generally vary linearly with salinity (Skwarzec, 1995). The average ^{238}U concentrations are 41.5±2.5 Bq m^{-3} (3.3±0.2 μg L^{-1}) in the open ocean (salinity normalized to 35.00 ‰) and 3.7±0.4 Bq m^{-3} (0.3±0.03 μg L^{-1}) in the major world rivers (Ku et al., 1977; Mangini et al., 1979; Owens et al., 2012). Therefore, the production of ^{234}Th is generally greater in the seaward portion of the estuary than in the landward part (Feng et al., 1999b). Furthermore, due to their short half-lives, ^{7}Be and ^{234}Th have proven to constitute a couple of excellent tracers to discern short-term variations in estuarine systems, such as flood deposition (Sommerfield et al., 1999; Mullenbach et al., 2004; Palinkas et al., 2005) and dynamic processes of particles and sediments (Olsen et al., 1986; Wallbrink and Murray, 1996; Feng et al., 1999a; Palinkas et al., 2005).

The Rhône subaqueous delta is a wave-dominated delta with micro-tidal influence and a pro-grading sedimentary structure (Syvitski and Saito, 2007), where resuspension occurs below 20 meter depths during large southeast storms occurring mostly in winter (Ulses et al., 2008; Dufois et al., 2014). Over the last two decades, numerous studies have been carried out to better understand the fate of particulate discharge from the Rhône River, especially during floods, in supplying terrigenous and river-borne material to the Mediterranean Sea and the flood impact on various processes (e.g., Milliams and Rose, 2001; Perianez, 2005; Maillet et al., 2006; Miralles et al., 2006; Lansard et al., 2007; Drexler and Nittrouer, 2008; Cathalot et al., 2010; Fanget et al., 2013). They revealed that a large majority of river particles discharged into the Mediterranean Sea are deposited, biogeochemically transformed and buried close to the Rhône River mouth in the pro-delta area. The transport and deposition of the remaining SPM is mainly diverted to the southwest in the Rhône River plume. Aloisi et al. (1979) showed that SPM carried by the Rhône towards the sea is stratified in a multi-layered system (surface plume, intermediate and benthic nepheloid layers). The surface plume can spread over several kilometers off

the river mouth during floods (Naudin et al., 1997; Thill et al., 2001). The intermediate layers are mainly seasonal while the benthic nepheloid layer is the thickest layer, which nourishes the prodelta, shelf and slope. Therefore, defining the preferential deposition area of river-borne particles and its initial repository is of particular interest to better understand the dynamics of riverine particles and their associated contaminants drained by the Rhône River into the Mediterranean Sea (Charmasson, 2003; Eyrolle et al., 2004; Roussiez et al., 2006, Radakovich et al., 2008).

The objective of our study is to define these initial particle deposition areas close to the Rhône River mouth labelled by ^{7}Be and ^{234}Th tracers, and to improve the understanding of short-term sedimentary processes in this area. It is important to document and understand the short-term deposition of riverine particles as it is strongly linked to the fate of the most labile part of the organic matter and the associated contaminants in these key regions at the land-sea interface constituted by river deltas.

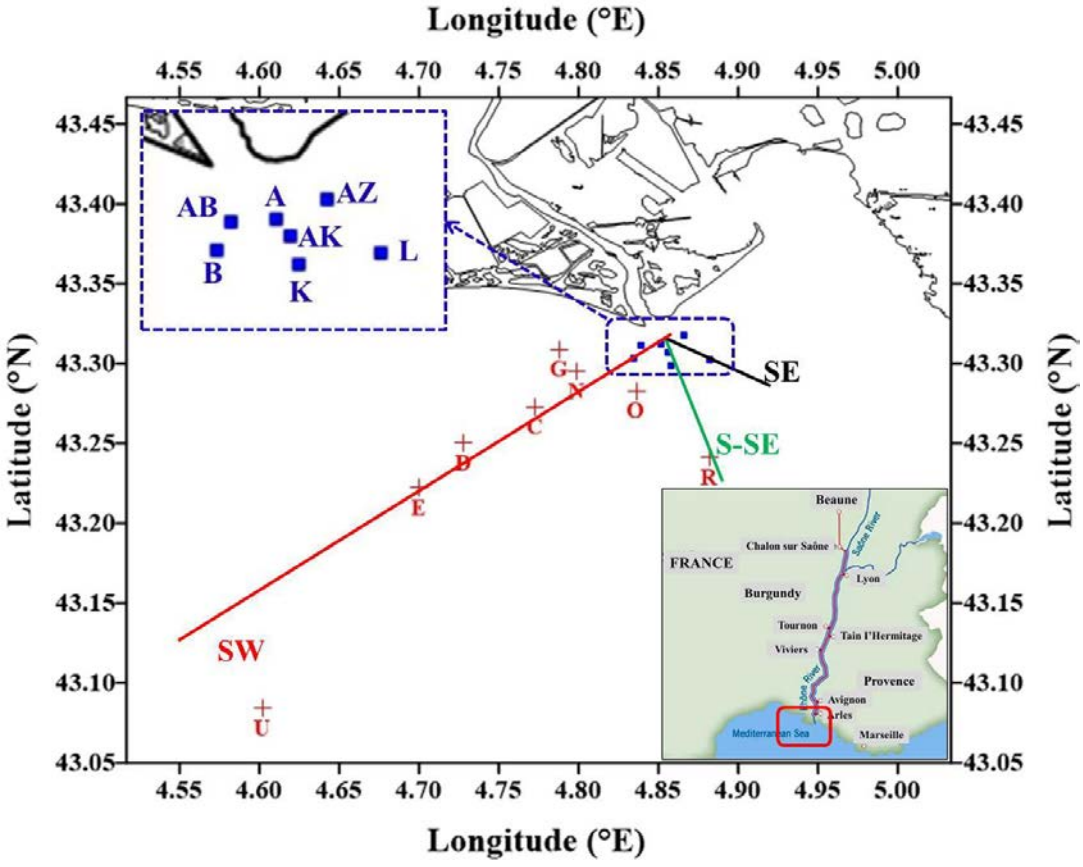

Figure 1. Maps of the Rhône River pro-delta showing the sampling locations

2. Materials and methods

2.1. Study area

The Rhône River, one of the largest rivers in France in terms of freshwater discharge, has a catchment area of about 98 000 km^2 and 832 km length and originates from the Alps. It flows into the Gulf of Lions (NW Mediterranean Sea) through a delta that comprises two branches, the Grand Rhône (carrying 90% of the mean water discharge) and the Petit Rhône (carrying the remaining 10%) (Ibanez et al., 1997). The Rhône River is the largest supplier of freshwater, sediments and nutrients to the Gulf of Lions and the western Mediterranean basin (De Madron et al., 2000; Sempéré et al., 2000; Pont et al., 2002; Sadaoui et al., 2016). The mean annual river discharge for the past sixty years was approximately 1720 m^3 s^{-1}. The values for the 1-year, 2-year, 10-year, 50-year, and 100-year return period (an estimate of the frequency of river flooding based on a stochastic concept) of high discharge correspond to 4000, 5000, 8400, 10400 and 11200 m^3 s^{-1}, respectively (Eyrolle et al., 2012 and references therein). The annual sediment discharge ranged from 0.98 to 19.7 million tons (Mt, $1Mt=1\times10^{12}$ g), with a mean discharge of 6.7 Mt over the period 1967-2008 (Pont et al., 2002; Eyrolle et al., 2012). Most of the solid load (>80%) comes from during flood events initiated in the mountainous portions of the Rhône River catchment (Pont et al., 2002; Antonelli et al., 2008). The Gulf of Lions, where the Rhône discharges, is micro-tidal with a tidal range of 30-50 cm (Dufois et al., 2008). Therefore, the Rhône estuary is stratified and tidal mixing is insignificant. A large turbid plume of one meter in thickness (occasionally up to 5 meters) with mixed freshwater and seawater extends offshore towards the southwest (Many et al., 2018). Below this layer, the salinity of the water is the Mediterranean seawater salinity, i.e., 38 ‰. As mentioned above, large resuspension events are limited to the winter and are generally weaker during spring, summer and fall, although occasional storms may displace centimetric layers of sediment (Toussaint at al., 2014; Dufois et al., 2014). The seafloor bathymetry in the subaqueous delta shows three major domains: the proximal domain, in a 2 km radius off the river mouth with water depth of 10-30 m; the pro-delta domain, 2-5 km off the river mouth with water depth ranging from 30 to 70 m; and the distal domain (continental shelf), beyond 5 km off the river mouth with water depth between 70 and 90 m (Got and Aloisi, 1990). The subaqueous delta

structure is characterized by fine-grained deposits in the proximal area below 20 meter depths (Durrieu de Madron et al., 2000; Roussiez et al., 2005). The net sedimentation rates varied from 30 to 50 cm yr^{-1} in the proximal domain (Calmet and Fernandez, 1990; Charmasson et al., 1998), to 1-2 cm yr^{-1} in the prodelta, down to 0.1-0.6 cm yr^{-1} with a mean rate of 0.3 cm yr^{-1} in the distal domain (Radakovitch et al., 1999; Miralles et al., 2005). The grain size in the entire area is quite homogeneous ($D_{0.5}$ =10-15µm) (Bonifacio et al., 2014; Cathalot et al., 2010). The biogeochemical characteristics are also very different between the three zones with large mineralization of organic matter involving sulfate reduction in the proximal and prodelta zones and suboxic diagenesis in the distal region (Pastor et al., 2011; Rassmann et al., 2016).

2.2. River discharge and SPM data

The Rhône River flow data was provided by the CNR (*Compagnie Nationale du Rhône*) and SPM was measured at the Arles-SORA station by the MIO (*Mediterranean Institute of Oceanology*). Daily SPM samples were obtained by automatically collecting 150 mL of water every 90 min. Samples for SPM analysis were preserved with $HgCl_2$ and stored at 5 °C until the bulk sample volumes were filtered using 1-µm pre-conditioned glass fiber filters (ashed at 450 °C for 4 h and pre-weighed before filtration). The SPM was quantified by differential weighing after drying at 60 °C for 24 h. The analytical uncertainty of SPM concentrations was 5×10^{-4} g L^{-1}.

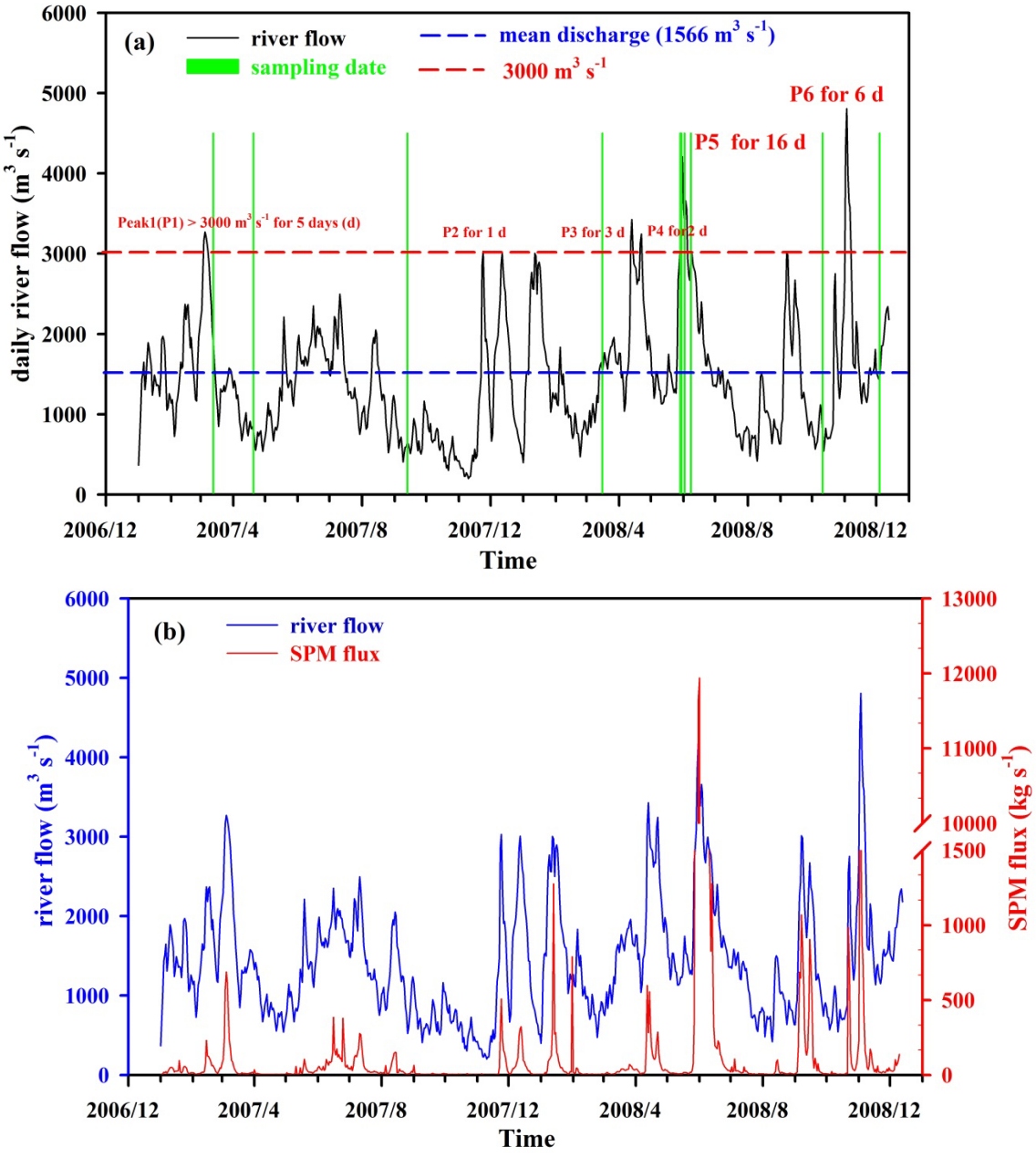

Figure 2. The daily variation of the Rhône River flow and the duration (in days) of river flooding during the sampling period (a) and the relationship between river flow and Suspended Particulate Matter (SPM) fluxes (b) during the period of 2007-2008.

2.3. Sample collection

The sediment cores were collected using various 20-40 cm corers that allow good preservation of the interface, i.e., Usnel box-corer and Octopus multi-corer, during seven

cruises conducted in the Gulf of Lions from March 13, 2007 to December 7, 2008 (Figure 1), a period characterized by a large and unusual flood in May-June 2008 created by a dam release on the largest alpine tributary (Durance) and a more typical flood in November 2008. Before the May-June 2008 flood, 21 sediment cores were collected in March, April and September 2007, and in March 2008. Five sediment cores were sampled off the Rhône River mouth during the 2008 flood (May-June), but only one core, Stn.AK3, was sampled after the main deposition event in the pro-delta. After the 2008 flood, six stations were sampled in October and December 2008. The detailed sample information is listed in Table 1. The sediment core samples were extruded onboard and sliced at depth intervals of 0.5-, 1.0- or 2.0-cm. Then, the subsamples were frozen and kept in that state until they were shipped to the shore-based laboratory, where they were dried (either at 60 °C for 24 h or freeze-dried) and pulverized using agate mortar and pestle sets.

2.4. ^{7}Be isotope measurement

The radionuclide measurements were carried out in two laboratories: "*Laboratoire Souterrain de Modane* (LSM)" in the French Alps (Reyss et al., 1995; Cazala et al., 2003) and "*Laboratoire de Mesure de la Radioactivité de l'Environnement* (LMRE)" in Orsay (IRSN) (De Vismes Ott et al., 2013). At LSM, 3-4 g aliquots were measured in the wells of very low-background and high-efficiency germanium detectors. Protected from cosmic radiation by 1700 m of rocks, a background as low as 0.5 counts per minute from 40 keV to 3000 keV was measured. Due to the short half-life, no standard for ^{7}Be was used at LSM and the efficiency-versus-energy curve was extrapolated between ^{137}Cs gamma ray at 662 keV and ^{40}K at 1460 keV to the 478 keV peak of ^{7}Be (Larsen and Cutshall, 1981). Generally, a counting time of one day for the deepest samples leads to precise data (uncertainty less than 10% for 2σ counting statistical error). At LMRE, 60 mL or 220 mL (~50-300 g) sediments were measured with the coaxial or semi-planar (HPGe) germanium detectors for 24-48 hours, with a relative efficiency of over 50%. Detectors were in a room shielded with 10 cm of low-background lead and 5 mm of electrolytic copper, located underground under a 3 m thick boron concrete slab (De Vismes Ott et al., 2013).

218 **Table 1.** Sample information from selected stations of the Rhône River pro-delta sediments

Stations	Samples	Lat. (°N)	Long. (°E)	Depth (m)	Collection date (dd-mm-yyyy)	Measurement length (cm)	Distance (km) [a)]	Inventory	Data from Lab
Southwest transect (SW)									
A	2007Chenal20m(-1)	43.311	4.853	28	13-03-2007	16	2.03	closed	IRSN/LMRE
	2007Chenal30m(-2)	43.313	4.855	27	13-03-2007	16	2.07	closed	IRSN/LMRE
	2007HChenal20m(-3)	43.311	4.851	28	15-03-2007	14	2.03	closed	IRSN/LMRE
	A	43.312	4.852	25	20-04-2007	16	2.06	closed	LSCE/LSM
	A2	43.313	4.851	19	13-09-2007	7	1.92	closed	LSCE/LSM
	2008Chenal30m	43.313	4.854	26	16-03-2008	15	2.03	closed	IRSN/LMRE
	A3	43.310	4.851	32	29-05-2008	16	2.24	open	LSCE/LSM
	A4	43.313	4.855	21	04-12-2008	12	2.07	open	LSCE/LSM
AB	2008US 14KB	43.312	4.835	26	16-03-2008	6	2.08	open	IRSN/LMRE
	2007US-Rous	43.310	4.841	27	15-03-2007	6	2.12	closed	IRSN/LMRE
	2008RbRousSub	43.310	4.842	27	11-10-2008	13	2.12	closed	IRSN/LMRE
AK	AK3	43.307	4.856	42	08-06-2008	38	2.70	closed	LSCE/LSM
	AK4	43.307	4.856	46	04-12-2008	30	2.70	closed	LSCE/LSM
AZ	2008US 04KB	43.318	4.866	25	15-03-2008	4	2.30	closed	IRSN/LMRE
B	B	43.303	4.836	56	20-04-2007	10	2.93	closed	LSCE/LSM
	B2	43.302	4.834	56	12-09-2007	7	3.07	closed	LSCE/LSM
G	G	43.309	4.788	48	27-04-2007	6	4.91	closed	LSCE/LSM
N	N	43.295	4.799	67	24-04-2007	5	5.14	closed	LSCE/LSM
C	C2	43.272	4.772	75	14-09-2007	4	8.51	closed	LSCE/LSM
	C3	43.274	4.776	75	30-05-2008	7	8.13	closed	LSCE/LSM
	C4	43.273	4.770	72	04-12-2008	7	8.54	closed	LSCE/LSM
D	D	43.250	4.728	74	23-04-2007	8	12.75	closed	LSCE/LSM
	D2	43.301	4.728	72	14-09-2007	4	9.75	closed	LSCE/LSM
E	E	43.222	4.700	75	21-04-2007	5	16.56	closed	LSCE/LSM
U	U3	43.084	4.602	90	02-06-2008	1.5	33.51	closed	LSCE/LSM
South transect (S)									

K	K	43.301	4.858	62	29-04-2007	9	3.38	closed	LSCE/LSM
	K4	43.296	4.852	67	03-12-2008	8	3.76	open	LSCE/LSM
O	O	43.283	4.836	79	24-04-2007	5	5.14	closed	LSCE/LSM
R	R2	43.241	4.882	98	28-04-2007	5	10.32	closed	LSCE/LSM
Southeast transect (SE)									
L	L	43.304	4.880	64	19-04-2007	7	4.15	closed	LSCE/LSM
	L3	43.303	4.883	65	01-06-2008	8	4.41	closed	LSCE/LSM
	L4	43.300	4.883	66	07-12-2008	6	4.63	closed	LSCE/LSM

a) This indicates the distance from the sampling station to the reference site (43.329°N, 4.842°E) in the Rhône River mouth.

Calibrations in energy, resolution and efficiency were carried out using standard sources (including ^{7}Be) prepared in the "*Laboratoire des Etalons et Intercomparaisons*" of the IRSN (LEI, under COFRAC accreditation), filled with an epoxide resin multi-gamma mixture source supplied by CERCA Inc (France). The ^{7}Be was measured via its peak at 477 keV of 10.44% emission intensity. ^{7}Be activities were all corrected for decay from the date of sample collection in this study, and expressed as Bq kg^{-1} of dry weight of sediment. The two laboratories regularly participate in inter-comparison exercises at national and international levels and are reference laboratories in France. The results show an overall agreement between the two techniques with less than 10% difference.

2.5. $^{234}Th_{ex}$ isotope analysis

The dried and homogenized samples were weighed and transferred to plastic counting geometries for non-destructive analysis of ^{234}Th using gamma spectrometry. At LSM, six standards were used to calibrate the gamma detectors for the determination of gamma emitters (Cazala et al., 2003). ^{234}Th activity was measured in both laboratories directly from its gamma photo-peak at 63.3 keV. A correction for gamma attenuation was applied and the self-adsorption coefficient for ^{234}Th was also determined according to the methods suggested by Cutshall et al. (1983), because significant self-absorption of gamma energy occurs below 295 keV. At LMRE, for this low-energy line (<100 keV), a transmission measurement was carried out to determine the attenuation coefficients of the samples in order to correct the measured activity of the self-attenuation phenomena, which may be significant for sediments, especially on large geometries (220 mL) (Lefèvre et al., 2003). In addition, ^{234}Th supported by its grandparent ^{238}U was determined by recounting the deepest layers in the core after approximately 5 months. The average activities measured in the second count were subtracted from the activities determined in the first counting session. This allows us to determine excess ^{234}Th activities (activities not supported by ^{238}U; denoted $^{234}Th_{ex}$). The counting time was at least 24 h, depending on the sample activity. The activities of the excess ^{234}Th ($^{234}Th_{ex}$) were all corrected for decay from the sampling date and expressed as Bq kg^{-1} of dry weight of sediment.

2.6. Calculation of ^{7}Be and $^{234}Th_{ex}$ inventories and SPM flux

Inventories of ^{7}Be and $^{234}Th_{ex}$ are useful parameters for assessing the deposition

process of SPM. In this study, ^{7}Be and $^{234}Th_{ex}$ inventories in dry sediments were calculated by summing their respective activities at each layer, according to the following formula (Wang and Yamada, 2005):

$$I = \sum_{i=1}^{N} \rho_s X_i A_i \quad (1)$$

where I represents the inventories of ^{7}Be or $^{234}Th_{ex}$ in the dry sediments (mBq cm^{-2}), N is the number of sampling layers, ρ_s is the solid phase dry density, X is the thickness of the sampling interval i (cm), and A is the activity of the sampled interval (Bq kg^{-1}). Uncertainties on inventories are the sum of the propagated error determined for each of the sampling intervals. In some cores, ^{7}Be or $^{234}Th_{ex}$ activities were still detected in the deepest sampled layers. Therefore, for these cores the activities in the un-sampled deepest layers were extrapolated by fitting an exponential equation applied to the existing field data, to allow estimates of completed (closed) inventories.

The annual SPM fluxes (SPM_a in kg) were calculated through the following equation (Eyrolle et al., 2012):

$$SPM_a = \sum_{t=1}^{t=n} \left(\left(SPM_{ct} + SPM_{ct+1} \right) / 2 \right) \bullet \left(\left(Q_t + Q_{t+1} \right) / 2 \right) \bullet \Delta T \quad (2)$$

where n is the number of samples collected during the year, SPM_{ct} represents the SPM concentration measured over a given period of time or at the time t (mg L^{-1}), Q is the average river flow during the sampling period (m^3 s^{-1}), and ΔT is the period of time between two continuous samples collected at times t and $t+1$ (s). In order to take into account the fact that sediment deposition integrates several deposition events, and to better link particulate inputs and sediment inventories on the same timescale, we also calculated the cumulated SPM fluxes over two half-lives before the sampling date for each radionuclide by summing the particle discharge over this period of time, namely, ~106 d for ^{7}Be and ~48 d for ^{234}Th. For time periods longer than two half-lives before the sampling period, the radionuclide inventory will have decreased by 75% and will contribute marginally to the overall inventory.

3. Results

3.1. Temporal variations of river flow rates and particulate discharge

Temporal variations of river flow rates and particulate discharges measured at the SORA station located on the Grand Rhône in Arles 40 km, upstream of the river mouth during the period 2007-2008 are presented in Figure 2. The mean annual river flow rate over our study period is 1566±834 $m^3 s^{-1}$, which is in the range of the mean value over the past sixty years (1720±982 $m^3 s^{-1}$). At the SORA station in Arles, a river flood event is defined as a river flow rate above 3000 $m^3 s^{-1}$ since this threshold corresponds to a breakdown in the relationship between the river flow and SPM concentrations indicating the initiation of sediment transport under flood conditions (Pont et al., 2002; Antonelli, 2002; Eyrolle et al., 2012). The year 2007 was defined as a "no flood" year with river flow only approaching or slightly exceeding 3000 $m^3 s^{-1}$ from March 4 to 9 and on November 24 (Figure 2a), and was characterized by a very low annual particulate discharge, i.e., 1.5 Mt. In contrast, the year 2008 was characterized by a succession of moderate floods with up to about 4000-5000 $m^3 s^{-1}$ (Eyrolle et al., 2012; Zebracki et al., 2015). Over our 2008 sampling period (ending on December 7, 2008), two main floods occurred (Figure 2b). The first and main flood in terms of duration started on May 28 and ended on June 12, 2008 (~16 d), and the second one occurred from November 2 to 7, 2008 (~6 d). However, the SPM concentrations observed in May-June 2008 are exceptionally high for such a moderate flood. A mean daily SPM concentration peak reaching 3356 mg L^{-1} was recorded on June 1, 2008, with daily maximum SPM fluxes reaching 11940 kg s^{-1}. It is estimated that this atypical flood event of anthropogenic origin induced the transfer of 4.7 Mt SPM into the sea over a 16 day period, mostly from the flushing of old sediment trapped in reservoirs and the erosion of the river banks, which contains unusually low short-lived radionuclides (Eyrolle et al., 2012) and old carbon (Cathalot et al., 2013). This flood event accounts for ~52% of the 2008 annual SPM fluxes (about 9.1 Mt) and represents by itself three times the 2007 annual SPM fluxes (~1.5 Mt) (Eyrolle et al., 2012). In contrast, the SPM flux (~0.4 Mt) induced by the November flood event that reached 4800 $m^3 s^{-1}$ (November 2 to 7, 2008) only accounted for ~4% of the 2008 annual SPM flux (Grand Rhône).

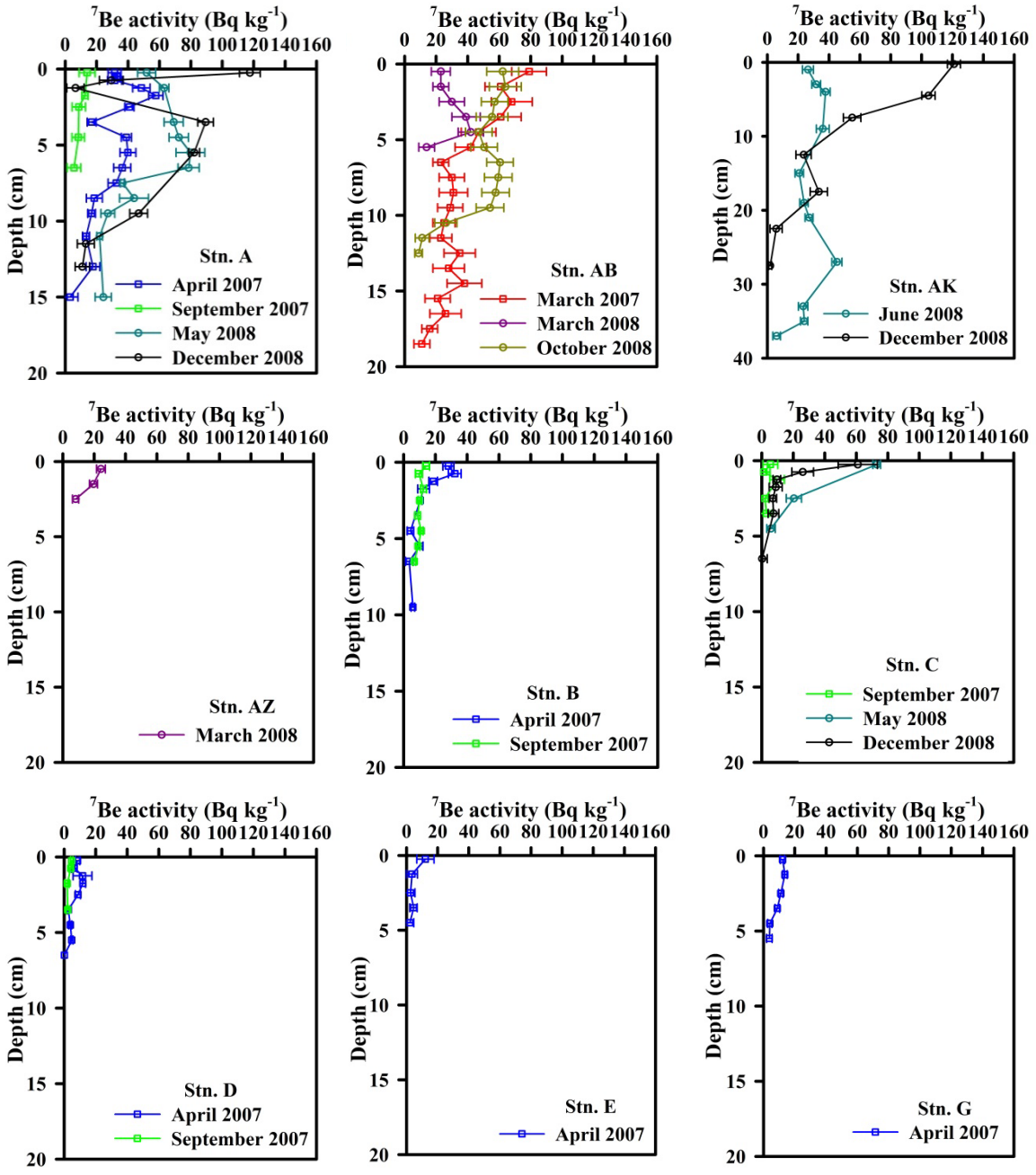
7Be activity (Bq kg-1)
Depth (cm)
Stn. A
April 2007
September 2007
May 2008
December 2008
Stn. AB
March 2007
March 2008
October 2008
Stn. AK
June 2008
December 2008
Stn. AZ
March 2008
Stn. B
April 2007
September 2007
Stn. C
September 2007
May 2008
December 2008
Stn. D
April 2007
September 2007
Stn. E
April 2007
Stn. G
April 2007

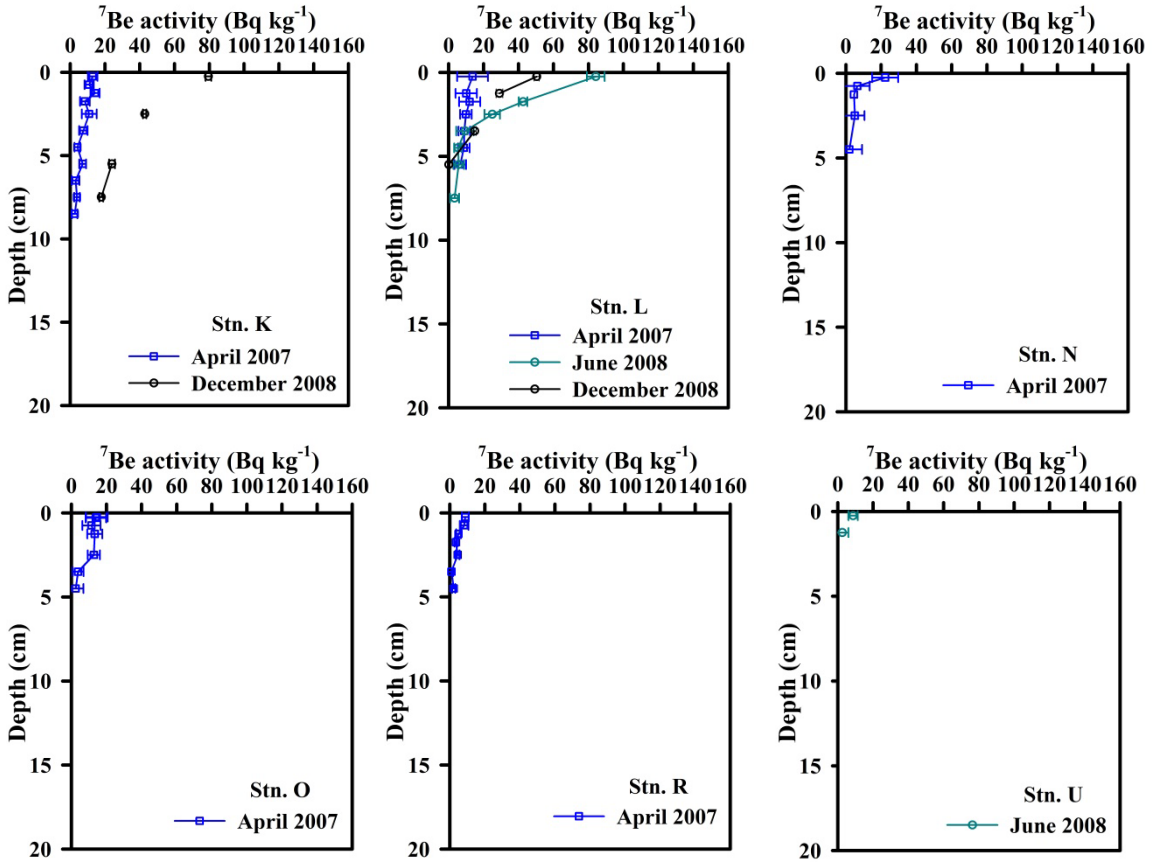

Figure 3. Vertical distributions of ^{7}Be activities in the sediment cores.

3.2. ^{7}Be activities and inventories

A selection of vertical distributions of ^{7}Be activities in the sediment cores are shown in Figure 3. Depth profiles of ^{7}Be activities in the sediment cores showed an overall decrease with depth, which is caused by burial, bioturbation and gradual decay of ^{7}Be with depth (Fitzgerald et al., 2001; Miralles et al., 2006). The ^{7}Be penetration depth also shows a decrease with increasing distance from the river mouth (from Stn.A to Stns. B, C, D, E and U).

Distributions of ^{7}Be activities in surface sediments demonstrate spatial and temporal variations. Spatial distributions showed a clear decrease of surface ^{7}Be activity with increasing distance from the river mouth. For example, in April 2007, along the SW direction, ^{7}Be activities at Stn.A adjacent to the river mouth were higher than at Stns. B, N and E.

^{7}Be inventories in the sediment cores are listed in Table 2 and they showed a large spatial variation with an 85-fold decrease from Stn.A in May 2008 (1826 mBq cm^{-2}) to Stn.U on the shelf (21 mBq cm^{-2}).

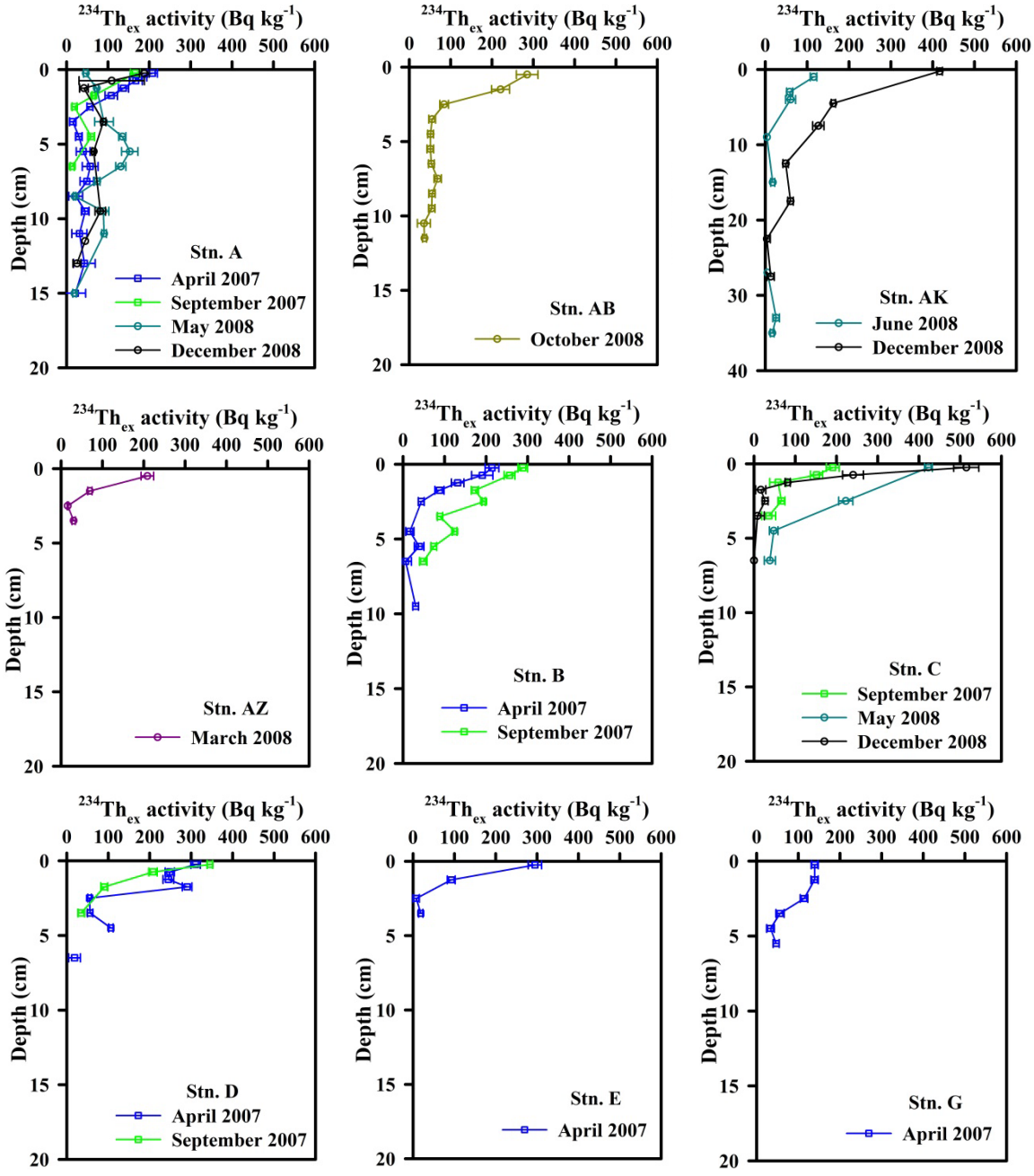

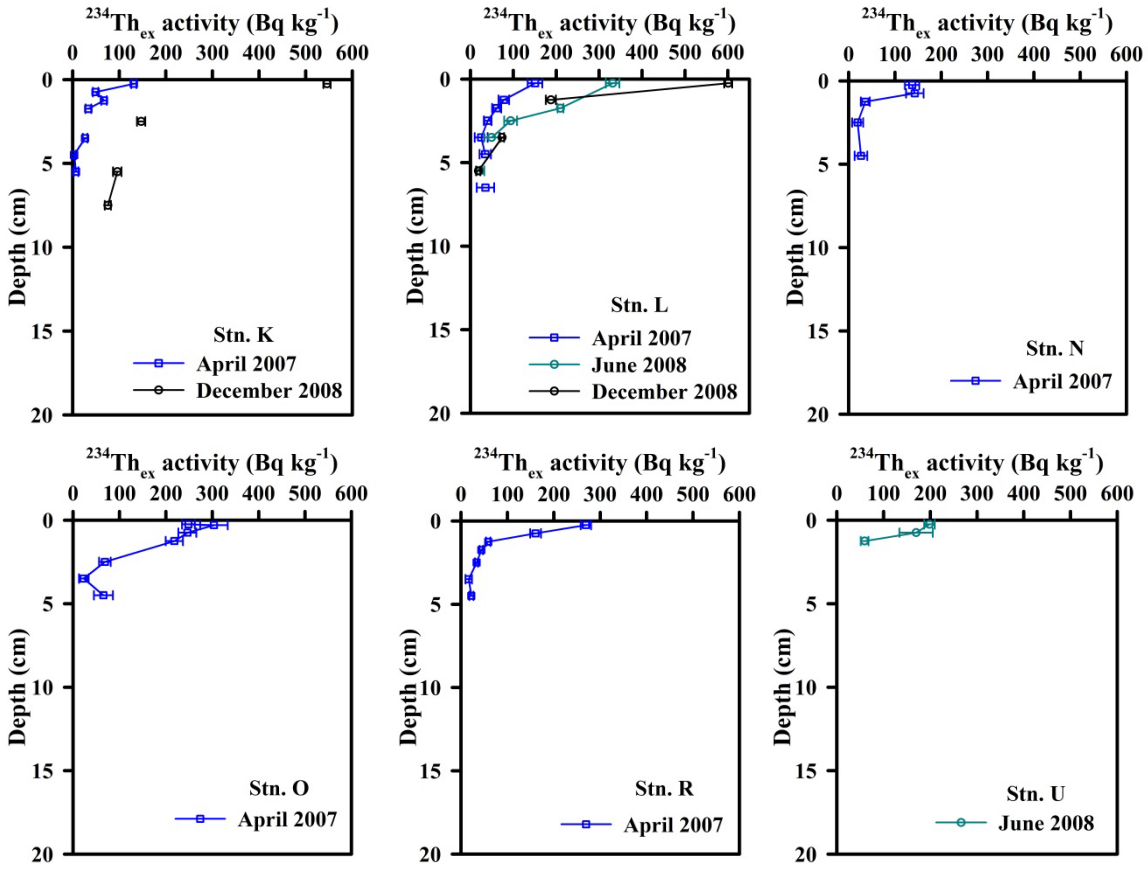

336

337

338

339 **Figure 4.** Vertical distributions of $^{234}Th_{ex}$ activities in the sediment cores.

340

341

342 ### 3.3. $^{234}Th_{ex}$ activities and inventories

343 Vertical distributions of $^{234}Th_{ex}$ activities in sediment cores also showed a decrease
344 with increasing depth (Figure 4). However, the horizontal distribution of surface activity
345 is inconsistent with that of ^{7}Be, since the $^{234}Th_{ex}$ activities in surface sediments did not
346 show a decrease with distance from the river mouth. Along the SW direction, the $^{234}Th_{ex}$
347 activity at Stn.E was higher than that of Stn.B close to the river mouth in April 2007.

348 **Table 2.** Inventories of ^{7}Be and $^{234}Th_{ex}$ in the Rhône River delta sediment cores and their $^{7}Be/^{234}Th_{ex}$ inventory ratios

Stations	Samples	Collection date (dd-mm-yyyy)	Cumulated SPM flux over 106 d (kg s^{-1})[a)]	Cumulated SPM flux over 48 d (kg s^{-1})[b)]	^{7}Be inventory (mBq cm^{-2})	$^{234}Th_{ex}$ inventory (mBq cm^{-2})	$^{7}Be/^{234}Th_{ex}$ inventory ratio
Southwest transect (SW)							
A	2007Chenal20m(-1)	13-03-2007	11080	5082	1915±306	4209±954	0.45±0.13
	2007Chenal30m(-2)	13-03-2007	11080	5082	1432±221	3055±362	0.47±0.09
	2007HChenal20m(-3)	15-03-2007	11013	5008	847±155	3715±597	0.23±0.06
	A	20-04-2007	6265	4296	940±175	2042±668	0.46±0.17
	A2	13-09-2007	7197	1518	163±43	1001±121	0.16±0.05
	2008Chenal30m	16-03-2008	6593	1281	277±29	1385±98	0.20±0.03
	A3	29-05-2008	9408	8336	1826±186	3081±348	0.59±0.09
	A4	04-12-2008	18364	10168	1963±155	2546±353	0.77±0.12
AB	2008US 14KB	16-03-2008	6593	1281	428±103	-	-
	2007US-Rous	15-03-2007	11013	5008	1735±428	-	-
	2008RbRousSub	11-10-2008	9350	8108	1537±260	2630±336	0.58±0.07
AK	AK3	08-06-2008	63216	59652	2797±275	2944±319	0.95±0.14
	AK4	04-12-2008	18364	10168	3064±289	5474±512	0.56±0.07
AZ	2008US 04KB	15-03-2008	6647	1268	130±18	814±65	0.16±0.03
B	B	20-04-2007	6265	4296	242±47	1294±292	0.19±0.06
	B2	12-09-2007	7204	1541	173±25	2496±137	0.07±0.01
G	G	27-04-2007	6101	895	134±21	1308±131	0.10±0.02
N	N	24-04-2007	6205	2169	74±23	599±196	0.12±0.06
C	C2	14-09-2007	7183	1496	41±32	837±142	0.05±0.04
	C3	30-05-2008	12919	11629	377±33	3000±204	0.13±0.01
	C4	04-12-2008	18364	10168	194±57	1156±153	0.17±0.05
D	D	23-04-2007	6215	2860	102±24	2118±159	0.05±0.01
	D2	14-09-2007	7183	1496	29±10	1237±83	0.02±0.01
E	E	21-04-2007	6268	3698	56±38	856±89	0.07±0.04
U	U3	02-06-2008	47852	45699	21±11	535±69	0.04±0.02
South transect (S)							

K	K	29-04-2007	5949	901	157±53	525±77	0.30±0.11
	K4	03-12-2008	18352	10149	741±23	3181±173	0.23±0.01
O	O	24-04-2007	6205	2169	113±51	1465±193	0.08±0.04
R	R2	28-04-2007	6052	712	52±15	850±76	0.06±0.02
Southeast transect (SE)							
L	L	19-04-2007	6278	3879	146±68	934±250	0.16±0.08
	L3	01-06-2008	35895	34019	459±70	2026±218	0.23±0.04
	L4	07-12-2008	18518	10352	294±13	2261±102	0.13±0.01

a) The cumulated SPM fluxes are calculated over 106 d (2 half-lives of ^{7}Be) before the sampling date.

b) The cumulated SPM fluxes are calculated over 48 d (2 half-lives of ^{234}Th) before the sampling date.

$^{234}Th_{ex}$ inventories in the sediment cores are also listed in Table 2. They varied from 525 to 5474 mBq cm^{-2}, showing a 10-fold decrease along the offshore transect. Within a 3 km area at the river mouth, $^{234}Th_{ex}$ inventories along the increasing distance from the river mouth varied from 2042±668 mBq cm^{-2} at Stn.A (2.1 km) to 1294±292 mBq cm^{-2} at Stn.B (2.9 km) in April 2007. During the same period, $^{234}Th_{ex}$ inventory (856±89 mBq cm^{-2}) at Stn.E (16.6 km) appears only slightly higher compared to Stn.N (599±196 mBq cm^{-2}) closer to the coast (5.1 km). When considering their uncertainty, $^{234}Th_{ex}$ inventories do not demonstrate a clear spatial variation as can be seen on ^{7}Be inventory distribution. This has to be related to the differences in primary sources: a point source from the mouth for ^{7}Be, while $^{234}Th_{ex}$ source is more spread out since it is produced in situ from dissolved uranium in saline water.

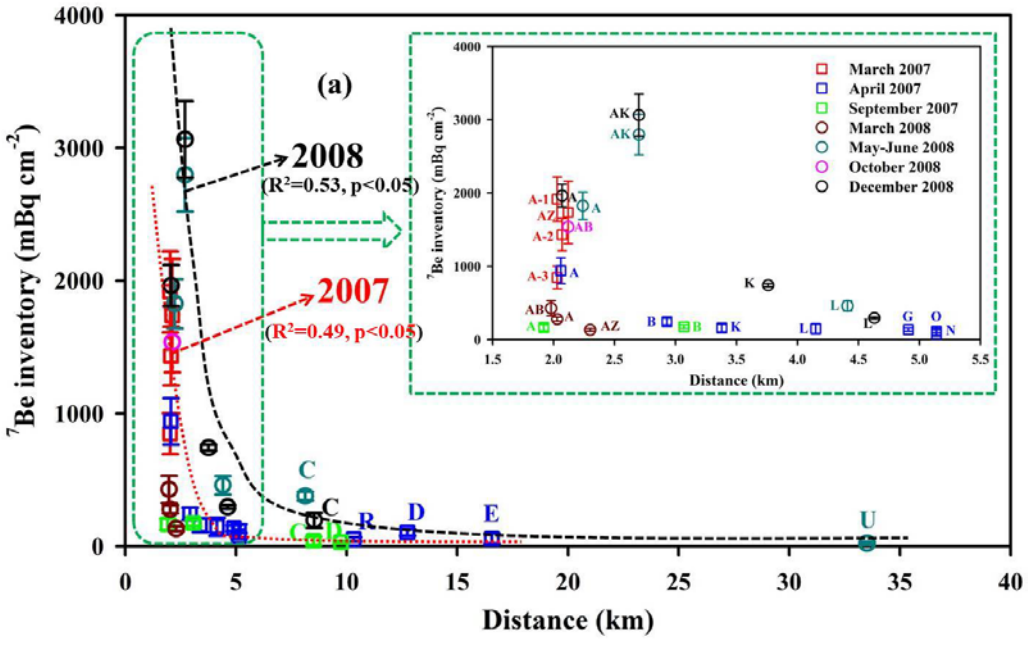

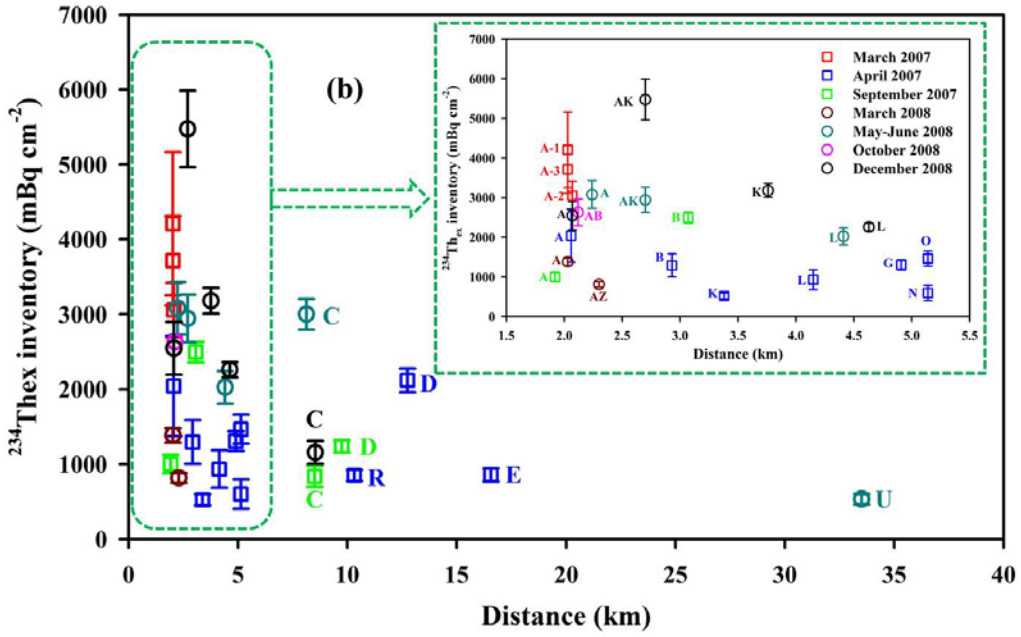

Figure 5. Inventories of ^{7}Be (a) and ^{234}Th$_{ex}$ (b) in the sediment cores, as a function of distance off the Rhône River mouth for March 2007 (red empty squares), April 2007 (blue empty squares), September 2007 (green empty squares), March 2008 (dark red empty circles), May-June 2008 (dark cyan empty circles), October 2008 (purple empty circles) and December 2008 (black empty circles). The exponential decreases of the ^{7}Be inventories with distance in 2007 and 2008 are plotted to highlight the trends.

4. Discussion

4.1. ^{7}Be and ^{234}Th$_{ex}$ as tracers of short term SPM deposition

SPM concentrations in surface water decrease rapidly seaward from 20 mg L^{-1} near the Rhône River mouth to 1.5 mg L^{-1} at the shelf break (Many et al., 2016). Given that ^{7}Be is largely associated with riverine particles, it thus follows the main riverine SPM deposition patterns. Therefore, the clear decrease in ^{7}Be activities with distance from the Rhône River mouth can be associated with the decreasing contribution of river-borne particles in offshore sediments. ^{7}Be inventories also showed an exponential decrease with increasing distance from the Rhône River mouth to shelf (seaward). The ^{7}Be inventories reach low values when the distance is over 5 km (see Figure 5a) and the highest ^{7}Be inventories appear within a ~5 km radius from the Rhône River mouth due to higher

activities and sediment penetration, indicating an important deposition of recent particles at these locations. The lower ^{7}Be inventories determined in sediments beyond 5 km off the river mouth indicate lower deposition rates or deposition of aged resuspended particles. Previous observations of the diffusive oxygen fluxes into the sediment (Lansard et al., 2009; Rassmann et al., 2016), organic carbon contents and chlorophyll-a concentrations in surficial sediments (Cathalot et al., 2010; Bourgeois et al., 2011) and other organic tracers (Cathalot et al., 2013) indicated similar gradients: the labile organic matter is deposited and mineralized near the river mouth, creating larger oxygen demand, and concentrations of chlorophyll-a with younger ^{14}C ages of organic matter whereas shelf sediments were characterized by lower oxygen demands and older organic material. In addition, we point out the variability in the ^{7}Be inventories obtained at Stn.A in March 2007 (847 to 1915 mBq cm^{-2}) (Table 2). This variability could be due to the fact that these cores were sampled in a channelized area characterized by high spatial variability in transport mechanisms (Maillet et al., 2006). Notwithstanding the variability at station A, the gradient between the proximal zone and the continental shelf is still very large with a 50-fold decrease between station A at lowest value and station U. It should also be noted that our two years study did not include many winter periods where significant resuspension events occur (Ulses et al., 2008).

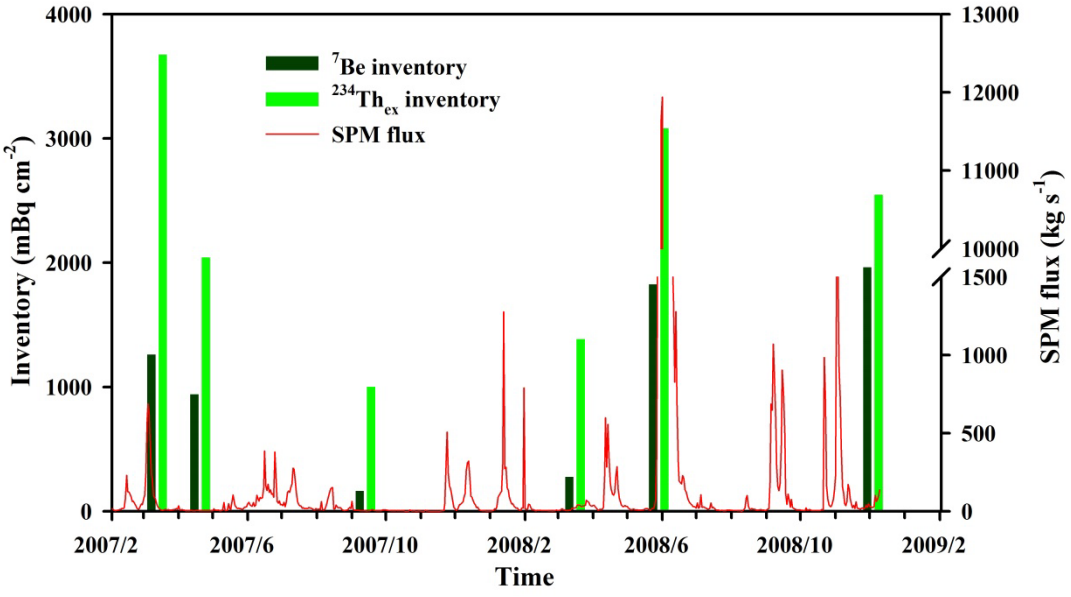

Figure 6. Temporal variations of ^{7}Be and ^{234}Th$_{ex}$ inventories at Stn.A.

Concerning $^{234}Th_{ex}$, high concentrations generally indicate a marine influence as it is produced by the decay of ^{238}U which is enriched in seawater. However, high $^{234}Th_{ex}$ activities are also observed near the Rhône River mouth. One reason could be the large amounts of riverine particles that would enhance $^{234}Th_{ex}$ scavenging from the saline part of the stratified water column at the river mouth (Corbett et al., 2004; McCubbin et al., 2004). Alternatively, the Rhône River could be an additional ^{234}Th source, as dissolved ^{238}U concentrations in the Rhône River are in the range of 7.5-20.0 Bq m^{-3} (0.6-1.6 μg L^{-1}). This is 2-5 times higher than the average concentration in the world rivers (3.7±0.4 Bq m^{-3}, 0.3±0.03 μg L^{-1}) (Ollivier et al., 2011), but lower than the average ^{238}U concentration of seawater in the Mediterranean Sea, which is ~43.2 Bq m^{-3} (~3.5 μg L^{-1}) (Delanghe et al., 2002). These high ^{238}U concentrations in the Rhône River water could be related to the lithological composition (carbonate rocks) of the Rhône basin (Ollivier et al., 2011) and agricultural fertilizers such as phosphates containing high ^{238}U used in the Rhône watershed (Eyrolle et al., 2012). Meanwhile, Zebracki et al. (2017) did not observe $^{234}Th_{ex}$ on SPM in the Lower Rhône River at the flow rates above 3000 m^3 s^{-1}. Therefore, the high ^{238}U concentration encountered in the river water allows the river to be a source of ^{234}Th limited to the Rhône prodelta.

$^{234}Th_{ex}$ inventories show a gradual decrease with increasing distance from the Rhône River mouth, and the highest $^{234}Th_{ex}$ inventories are also observed within a ~5 km radius off the river mouth (Figure 5b). However, high $^{234}Th_{ex}$ inventories are still observed beyond a ~5 km radius off the Rhône River mouth, such as at Stns. C (3000 mBq cm^{-2}) and D (2118 mBq cm^{-2}), which is different from the pattern of ^{7}Be. Such a difference in $^{234}Th_{ex}$ and ^{7}Be inventory distribution can be mainly attributed to their different source terms, i.e., ^{7}Be source derived mainly from the river, while the $^{234}Th_{ex}$ is linked to in situ production in saline water (Saari et al., 2010).

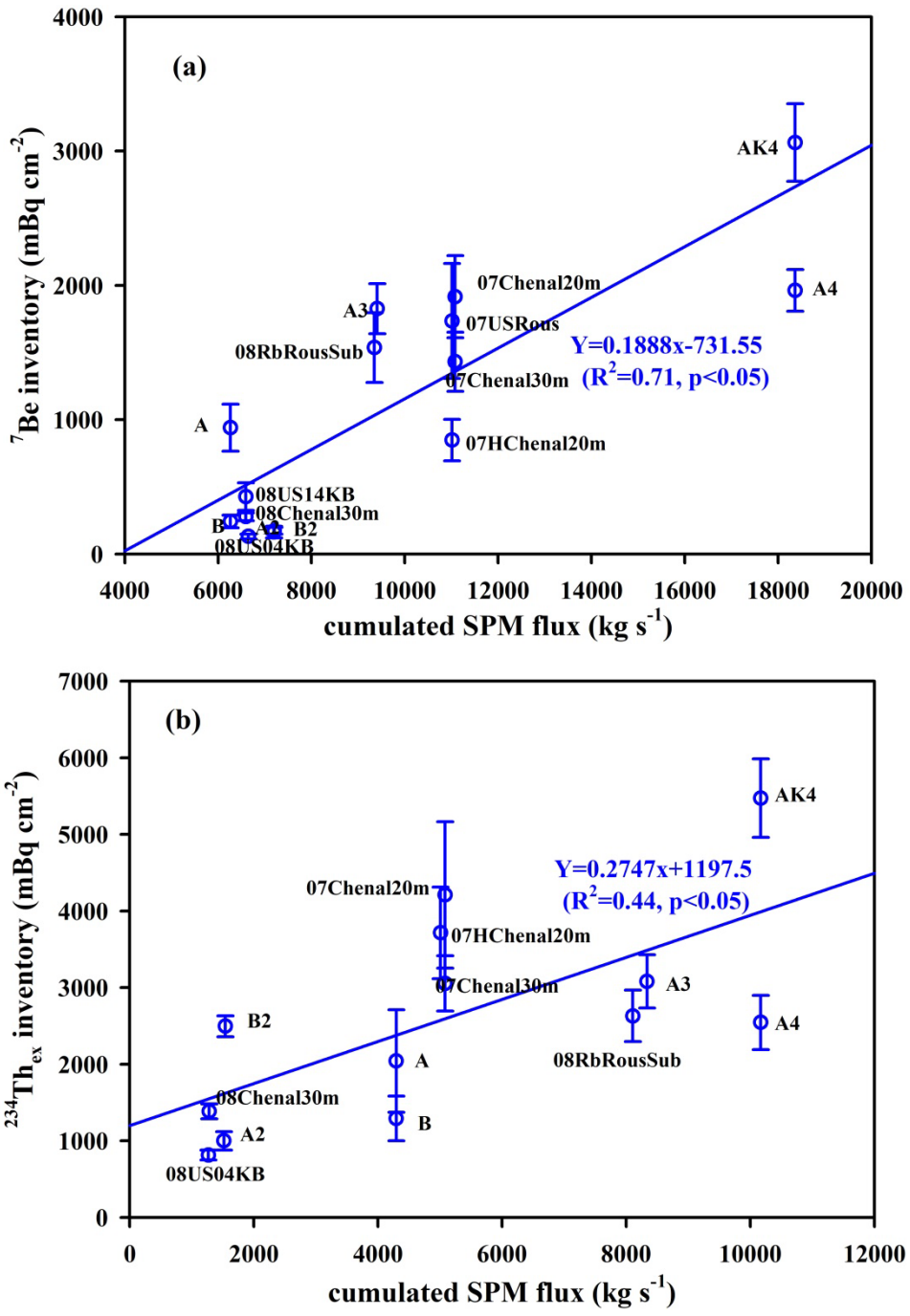

Figure 7. Relationship between ^{7}Be inventories in the Rhône River pro-delta and cumulated SPM fluxes calculated over 106 d (2 half-lives of ^{7}Be) before the sampling date (a) excluding the Stn.AK3 collected during May-June 2008 flood; and relationship between the ^{234}Th$_{ex}$ inventories in the Rhône River pro-delta and cumulated SPM fluxes calculated over 48 d (2 half-lives of ^{234}Th) before the sampling date (b), excluding Stn.AK3.

4.2. Relation of ^{7}Be and $^{234}Th_{ex}$ with river particulate flux

Large temporal variations in ^{7}Be activities near the river mouth (Stns. A, AB, AK) appeared to be associated with river particulate discharge. In general, high river particulate discharge corresponds to high ^{7}Be activities in proximal zone sediments. For example, at Stn.A, ^{7}Be activities in December 2008 were higher than in March 2008 since the river particulate discharge in December 2008 was also higher compared to March 2008. Like ^{7}Be, $^{234}Th_{ex}$ activities (Table 2) also seem to demonstrate a positive relationship with the river particulate discharge (R^2=0.26, $p<0.05$). For example, at Stn.A, $^{234}Th_{ex}$ activities (Table 2) observed in March 2007 are higher than in September 2007 when the SPM flux is lower. Indeed, at this station, the periods of high ^{7}Be and $^{234}Th_{ex}$ inventories were associated with higher river flow and river particle discharge. High SPM riverine fluxes in March 2007 and December 2008 led to higher ^{7}Be and $^{234}Th_{ex}$ inventories compared to those observed in September 2007 and March 2008 when SPM fluxes were lower (Table 2). This correlates with a study on the western shelf of the Mississippi River delta carried out by Corbett et al. (2007), where high ^{7}Be inventories near the Mississippi River mouth were positively associated with river particulate discharge. Similar time variations of ^{7}Be and $^{234}Th_{ex}$ inventories were also observed in other estuarine systems, such as the Tampa Bay (Baskaran and Swarzenski, 2007), Gironde estuary (Saari et al., 2010) and Yangtze River estuary (Wang et al., 2016).

High inventories of short-lived radionuclides in the sediment indicate high recent deposition of particles near the river mouth and most definitely preferential deposition and accumulation of sediment. Indeed, apparent accumulation rates studied in the same areas with longer half-life radionuclides such as ^{137}Cs or ^{210}Pb (Calmet and Fernandez, 1990; Charmasson et al., 1998; Radakocitch et al., 1999) also show large sedimentation rates near the Rhône River mouth with very high values around 30-50 cm yr^{-1} and a gradual decrease with increasing distance from the shoreline. Certainly, this apparent consistency between inventories and apparent accumulation rates does not imply that once settled the bottom particles do not undergo resuspension/transport processes since this area can be very dynamic during storm events, especially during the winter (Marion et al., 2010; Dufois et al., 2014).

As we have seen, the activities and inventories of ^{7}Be and $^{234}Th_{ex}$ are only qualitatively related to river particulate discharges. This is due to the integrative timescale of sediment inventory (which spans over a few half-lives of the radionuclides) versus the instantaneous time frame captured by the daily particulate discharge. To bridge this time lag, we have integrated the SPM fluxes over the period preceding the sampling date and compared it to the sediment inventory. The integration period covering two half-lives before the sampling date was chosen, i.e., 106 days for ^{7}Be and 48 days for $^{234}Th_{ex}$ (see in the Materials and Methods section). The cumulated SPM fluxes calculated accordingly are listed in Table 2 and compared with the ^{7}Be inventory in sediments (Figure 7a).

Before discussing the correlations, it is worth noting that the SPM concentration in the 2008 May-June flood is similar to the major flood in December 2003 (3669 mg L^{-1} for a flow rate of about 10000 m^3 s^{-1}: Eyrolle et al., 2012). This atypical high particulate load is linked to the upper Durance dam management, which discharged the excess water after heavy precipitation events into the southeastern Rhône watershed (Eyrolle et al., 2012). Therefore, the Stn.AK3 (close to the river mouth and sampled after the May-June flood) is very peculiar due to the nature of the transported solid load, which was characterized as “old” material (Cathalot et al., 2013) consequently depleted in short half-life radionuclides (Eyrolle et al., 2012). Accordingly, the highest cumulated SPM flux corresponds to low short-lived radionuclide activities, resulting in lower inventories than those expected under typical flood conditions (see a broader discussion of this atypical flood in Eyrolle et al., 2012). When data from this atypical flood (Stn.AK3) were excluded, ^{7}Be inventories show a good correlation with the cumulated SPM flux (R^2=0.71, $p<0.05$), indicating that the ^{7}Be inventory is a fair record of the riverine particles deposition on a timescale of 3-4 months.

The highest $^{234}Th_{ex}$ inventories were observed in the river mouth, such as at station A. This suggests that: 1) $^{234}Th_{ex}$ generated by both seawater and the Rhône water was carried by particles towards the river delta (Ollivier et al., 2011); 2) the scavenging of $^{234}Th_{ex}$ was enhanced because freshwater mixing with marine water led to high turbidity and sedimentation rates (aggregation and flocculation processes) in this area. Through 12-year observations (1988-2000), Corbett et al. (2004) also pointed out that the $^{234}Th_{ex}$ inventories in the Mississippi River estuary are positively correlated with river particulate

discharge. $^{234}Th_{ex}$ inventories also seem to be related to Rhône River particulate discharge although the relationship with cumulated SPM fluxes over ~48 days before the sampling appears to be much weaker compared to ^{7}Be (R^2=0.44, $p<0.05$) (Figure 7b). As mentioned above, this is likely linked to their difference in source terms, which are mainly riverine for ^{7}Be and both riverine and marine for $^{234}Th_{ex}$. The ^{7}Be and $^{234}Th_{ex}$ particulate activities in the lower Rhône River ranged from 15 to 400 Bq kg^{-1} and from unquantifiable to 56±14 Bq kg^{-1}, respectively (Eyrolle et al., 2012; Zebracki et al., 2017). Despite the dual nature of $^{234}Th_{ex}$, the different sources allow us to define a zoning with respect to the influence of the Rhône River particulate discharge.

4.3. Zoning of the Rhône River influence on sediments

^{7}Be and $^{234}Th_{ex}$ are both strongly bound to particulate matter, without significant difference in preferential adsorption (K_d) at high SPM concentrations, such as in the river mouth (Baskaran et al., 1997; Baskaran and Swarzenski, 2007). The potential differences in their specific activities and inventories are mainly caused by source terms, seasonal variations of the river particulate discharge, grain size, distance of salt-water intrusion and amounts of particles in the water column (Feng et al., 1999a; Saari et al., 2010). Figure 5a clearly shows two populations of ^{7}Be inventories with large and variable values near the river mouth at stations A and AB (or AZ) which are the closest stations to the river mouth and lower values further on the shelf. It must be noted that the two possible explanations of Figure 5a (i.e., two separate inventory populations or gradual decrease offshore of the inventories) support the zoning based on $^{7}Be/^{234}Th_{ex}$ inventory ratio. The decrease in ^{7}Be inventory offshore is persistent in time and the trend lines for 2007 and 2008 show good statistics (R^2=0.49 and 0.53) which lend support to a rapid decrease of ^{7}Be activity offshore. ^{7}Be is thus a powerful tracer for riverine particles although ^{7}Be-deficient sediments were exceptionally discharged by the Rhône River into the sea during the May flood event of 2008 due to rapid erosion of old watershed sediments. The situation is less clear for $^{234}Th_{ex}$ as a tracer of marine influence with more variable inventory at and near the river mouth, but a decrease offshore, although much weaker than ^{7}Be, is also visible (Figure 5b). Notably, this weak decrease of ^{234}Th inventories from the mouth of the river towards the shelf in the Rhône River deltaic region is

contrary to expectations if ^{234}Th is assumed to have only a marine source. The large spread observed in both radionuclides inventory is due to different source inputs, change in grain size and sediment type (Feng et al., 1999a, b). The use of ^{7}Be/^{234}Th$_{ex}$ inventory ratio may allow avoiding these inventory variations and be a better indicator than ^{7}Be alone. It is noteworthy that, in other cases such as the Mississippi River deltaic region where ^{234}Th$_{ex}$ inventories increase with the distance off the river mouth (Corbett et al., 2004), the use of ^{7}Be/^{234}Th$_{ex}$ inventory ratio is more powerful than the single radionuclide ^{7}Be.

The ^{7}Be/^{234}Th$_{ex}$ inventory ratios in sediment ranged from 0.02 to 0.77, with large variations with the distance from the Rhône mouth (Figure 8). The ^{7}Be/^{234}Th$_{ex}$ inventory ratios decreased from 0.59 at Stn.A3 (32 m water depth) to 0.04 at Stn.U (90 m water depth) in June 2008, and from 0.77 (21 m water depth) at Stn.A4 to 0.17 at Stn.C (72 m water depth) in December 2008. The lowest ratio of 0.04 indicates that the riverine source traced by ^{7}Be has disappeared and that the marine influence is dominant. In contrast, the high ratio of 0.77 indicates that the riverine source is dominant. High ^{7}Be/^{234}Th$_{ex}$ inventory ratios also mainly occur within a ~ 5 km radius off the river mouth. Feng et al. (1999b) pointed out that the ^{7}Be/^{234}Th$_{ex}$ inventory ratios are a negative function of both the water depth and salinity in a completely different context of a partially-mixed tidal estuary, namely, increasing with the decrease of water depth and salinity. However, the Rhône River plume spreads over several kilometers off the Rhône mouth and the low salinity waters are confined to a thin surface layer at the surface with seawater below the plume (Naudin et al., 1997; Arnoux-Chiavassa et al., 2003; Many et al., 2016), indicating that the impact of salinity on the ^{7}Be/^{234}Th$_{ex}$ inventory ratio can be ruled out. Thus, in our case, the ^{7}Be/^{234}Th$_{ex}$ inventory ratio is negatively correlated with water depth.

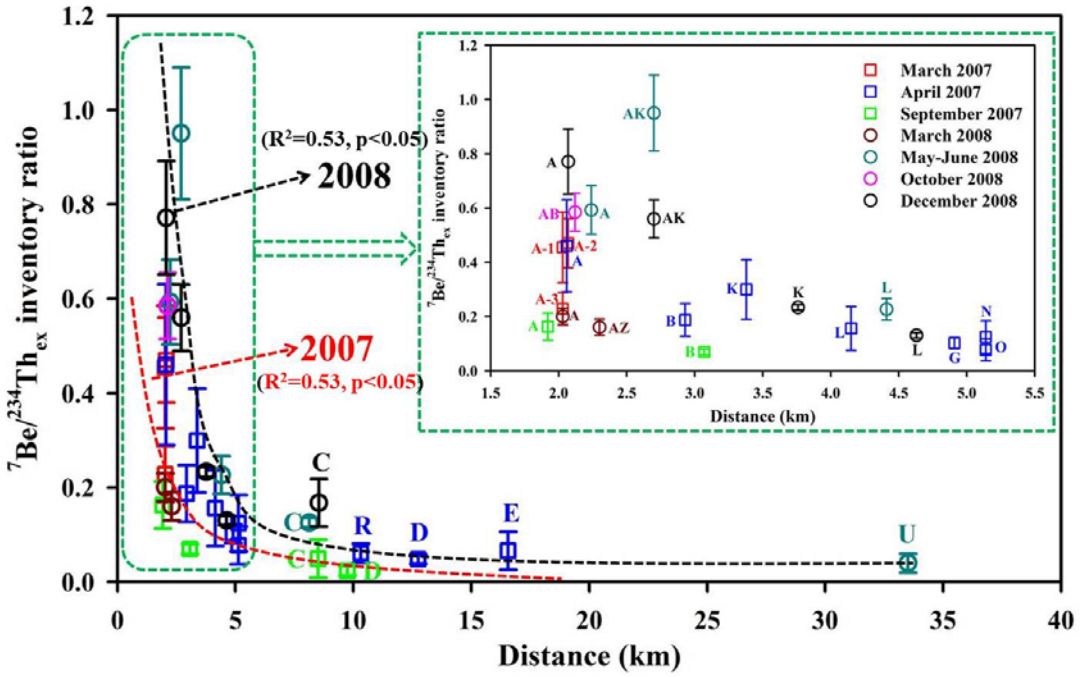

Figure 8. $^{7}Be/^{234}Th_{ex}$ inventory ratio in sediment cores as a function of distance from the Rhône River mouth for March 2007 (red empty squares), April 2007 (blue empty squares), September 2007 (green empty squares), March 2008 (dark red empty circles), May-June 2008 (dark cyan empty circles), October 2008 (purple empty circles) and December 2008 (black empty circles). The exponential decreases of $^{7}Be/^{234}Th_{ex}$ inventory ratios with distance off the Rhône River mouth in 2007 and 2008 are plotted to highlight the trends.

The $^{7}Be/^{234}Th_{ex}$ inventory ratios also show temporal variations and are mainly related to river particulate discharge, especially close to the river mouth. The $^{7}Be/^{234}Th_{ex}$ inventory ratios from 2008 are overall higher than in 2007. The $^{7}Be/^{234}Th_{ex}$ inventory ratios also demonstrated an overall positive correlation with the river particulate discharge, from normal discharge to flood discharge. At Stn.A, the $^{7}Be/^{234}Th_{ex}$ inventory ratios in December 2008 (influenced by the November flood) are higher than in March 2008, when the discharges were lower and resuspension during the end of the winter may have redistributed part of the deposited particles. In addition, as already reported, SW preferential deposition is visible in our data set. In this direction, at Stn.C (8.5 km away from river mouth), the $^{7}Be/^{234}Th_{ex}$ inventory ratios in December 2008 were three times

larger than in April 2007, showing that this station is impacted by newly deposited particles. However, in the SE direction at Stn.L (4.5 km), the $^{7}Be/^{234}Th_{ex}$ inventory ratio displays lower values. This feature is clearly consistent with the dominant spread direction of the Rhône River plume, generally in a SW direction, which has been proven to be the preferential direction for deposition of the riverine material in this area (Naudin et al., 1997). Similar patterns have already been reported for other tracers, such as trace metals (Alliot et al., 2003; Roussiez et al., 2006; Radakovitch et al., 2008), man-made radionuclides (Calmet and Fernandez, 1990; Charmasson, 2003; Lansard et al., 2007), and carbon and nitrogen stable isotopes (Lansard et al., 2009; Cathalot et al., 2013).

Table 3. Zoning in the Rhône pro-delta, where is dominant between riverine and marine influences

Zone	Distance (km)	$^{7}Be/^{234}Th_{ex}$ inventory ratio	River vs. Marine
I	< 3.0	>0.50	River
II	3.0~8.5	0.10~0.50	River & Marine
III	>8.5	<0.10	Marine

The use of the $^{7}Be/^{234}Th_{ex}$ inventory ratio allowed us to establish a zoning regarding the particle deposition with the distance from the Rhône River mouth. In order to examine if $^{7}Be/^{234}Th_{ex}$ inventory ratios have a significant difference in the different zones, we applied a simple Mann-Whitney U test (Fay and Proschan, 2010). Close to the Rhône River mouth, at a distance of less than 3.0 km, such as for Stns. A, AB and AK4, defined as Zone I (surface area near river mouth ~7 km^2), $^{7}Be/^{234}Th_{ex}$ inventory ratios, ranging from 0.16 to 0.95, display a significant difference ($p<0.05$) with the values obtained at a larger distance. These correspond to the continental shelf (distance from the river mouth >8.5 km), with stations D, E, R and U designated as Zone III (surface area off river mouth >150 km^2), with $^{7}Be/^{234}Th_{ex}$ inventory ratios ranging from 0.02 to 0.07. This indicates that the inputs of river-borne particles are dominant in Zone I, while Zone III is characterized by a stronger marine particle influence. At an intermediate zone with Stns. AZ, B, C, G, K, L, N, and O (defined as Zone II, distance from the river mouth =3.0-8.5 km), the $^{7}Be/^{234}Th_{ex}$ inventory ratios are between 0.05 and 0.30 suggesting a

mixed influence of particles labelled by river and seawater, recently deposited in this area. The zoning based on inventory ratios is presented in Figure 9 and summarized in Table 3.

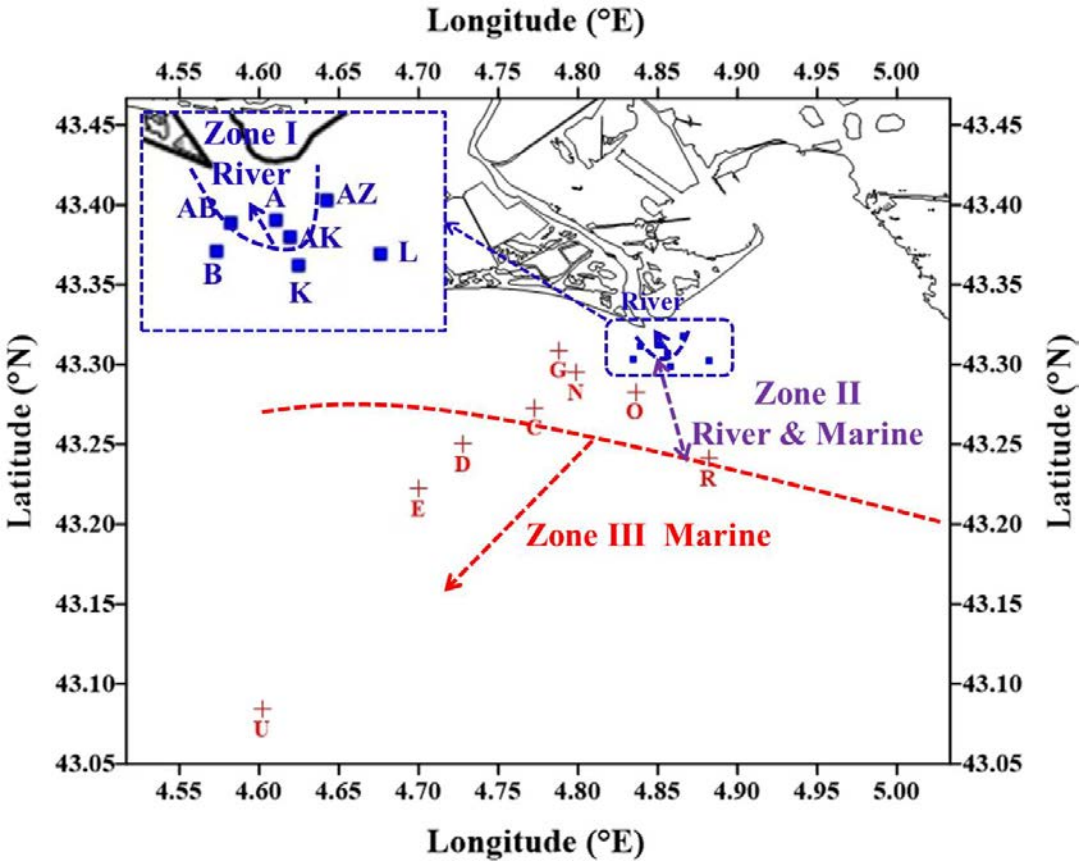

Figure 9. The zoning with different dominant sources of particles: input of river-borne particles (River) near the river mouth and marine particles (Marine) on the continental shelf.

This zoning is comparable to the observation by Rassmann et al. (2016), who demonstrated that the average oxygen penetration depth into Zone I sediment was one fifth of that in Zone III. In addition, Zone I, which corresponds mainly to the pro-deltaic area, appears to be the area where most of the particle associated contaminants driven by the Rhône River into the Gulf of Lions are deposited (Miralles et al., 2004; Roussiez et al., 2005). This zoning is therefore helpful for further understanding the spreading of particles-associated contaminants, such as man-made radionuclides and heavy metals (Charmasson et al., 1998; Radakovitch et al., 2008; Ferrand et al., 2012), and its initial sedimentary deposition in the Gulf of Lions. This study provides an effective reference to assess riverine and marine influence beyond the Rhône, which is very important for

understanding the initial deposition of riverine particles as tracking the recent particles deposition on the time scale of a few months has been rarely performed in deltas and estuaries.

5. Conclusions

Short-term deposition of particles close to the Rhône River mouth in the Gulf of Lions was traced by natural radionuclides ^{7}Be and $^{234}Th_{ex}$. Both the ^{7}Be and $^{234}Th_{ex}$ inventories are larger at the Rhône River mouth and were correlated with cumulated SPM fluxes calculated over two half-lives before the sampling date. The spatial distributions of ^{7}Be inventories and $^{7}Be/^{234}Th_{ex}$ inventory ratios showed an exponential decrease with distance from the river mouth. Their distributions indicated that recent particles are mainly deposited within a ~5 km radius from the river mouth and that maximal deposition occurs within 3 km off the river mouth. These areas of recently deposited particles coincide with areas with high apparent accumulation rates determined using ^{137}Cs or $^{210}Pb_{ex}$. Moreover, the gradients in the sediment $^{7}Be/^{234}Th_{ex}$ inventory ratio observed in the studied area lend support to the notion that this ratio can be used as a potential index for identifying the dominant influence between the river and the sea on the deposited particles. The riverine and marine influences can be classified as follows: Zone I (distance from the river mouth < 3.0 km with $^{7}Be/^{234}Th_{ex}$ inventory ratio over 0.50, surface area near river mouth ~7 km^2) is dominated by riverine input, while Zone III (distance from the river mouth beyond 8.5 km with $^{7}Be/^{234}Th_{ex}$ inventory ratio less than 0.10, surface area off river mouth beyond 150 km^2) is under a marine influence. In between, the transition zone (Zone II, distance from the river mouth: 3.0-8.5 km with $^{7}Be/^{234}Th_{ex}$ inventory ratios between 0.10 and 0.50) displays a mixed influence.

Author information

*** Corresponding authors:**

Tel: +33-4-94-30-48-29, Fax: +33-4-94-30-44-16 (S. Charmasson).

E-mail: christophe.rabouille@lsce.ipsl.fr (C. Rabouille).

sabine.charmasson@irsn.fr (S. Charmasson).

Notes

The authors declare that there is no competing financial interest.

Author Contributions

The manuscript was written through contributions from all authors. All authors have given approval to the final version of the manuscript.

Acknowledgements

This work was supported by the AMORAD project (French state financial support managed by the National Agency for Research allocated in the “Investments for the Future” framework program under reference ANR-11-RSNR-0002), and STU Scientific Research Foundation for Talents (NTF18011). Funding was also provided by the Midi Pyrénées-Paca Interregional Project CARMA, ANR-EXTREMA, ANR-CHACCRA the EC2CO Riomar.fr, and Mistrals/Mermex through the “Mermex-Rivers” action. We thank the captains and crews of the R.V. Europe and Tethys II for their collaboration during the sampling expeditions. We deeply thank Mireille Arnaud, chief scientist of the CARMEX (March 2007) and Extrema1 (March 2008) cruises. We are very grateful to *Compagnie Nationale du Rhône* and *MOOSE/SORA observatory* in Arles for providing freshwater discharge and particle load data, respectively. Three anonymous reviewers are thanked for their constructive comments and suggestions that have contributed to improve this paper.

References

Aller, R.C., Cochran, J.K., 1976. $^{234}Th/^{238}U$ disequilibrium in near-shore sediment: particle reworking and diagenetic time scales. Earth Planet. Sci. Lett. 29, 37-50.

Alliot, E., Younes, W.A., Romano, J.C., Rebouillon, P., Masse, H., 2003. Biogeochemical impact of a dilution plume (Rhône River) on coastal sediments: comparison between a surface water survey (1996-2000) and sediment composition. Estuar. Coast. Shelf Sci. 57, 357-367.

Aloisi, J.C., Millot, C., Monaco, A., Pauc, H., 1979. Dynamique des suspensions et mecanismes sedimentologiques sur le plateau continental du Golfe du Lion. C.R. Acad. Sci. Paris D 289, 879-882.

680 Antonelli, C., 2002. Flux sedimentaires et morphogenese recente dans le chenal du Rhône
681 aval. Universite de Provence, Aix en Provence, pp 272.
682 Antonelli, C., Eyrolle, F., Rolland, B., Provansal, M., Sabatier, F., 2008. Suspended
683 sediment and ^{137}Cs fluxes during the exceptional December 2003 flood in the Rhône
684 River, southeast France. Geomorphology 95, 350-360.
685 Arnoux-Chiavassa, S., Rey, V., Fraunie, P., 2003. Modeling 3D Rhône River plume using
686 a higher order advection scheme. Oceanol. Acta 26, 299-309.
687 Baskaran, M., Ravichandran, M., Bianchi, T.S., 1997. Cycling of ^{7}Be and ^{210}Pb in a high
688 DOC shallow, turbid estuary of south-east Texas. Estuar. Coast. Shelf Sci. 45, 165-176.
689 Baskaran, M., Swarzenski, P.W., 2007. Seasonal variations on the residence times and
690 partitioning of short-lived radionuclides (^{234}Th, ^{7}Be and ^{210}Pb) and depositional fluxes
691 of ^{7}Be and ^{210}Pb in Tampa Bay, Florida. Mar. Chem. 104, 27-42.
692 Bianchi, T.S., Allison, M.A., 2009. Large-river delta-front estuaries as natural “recorders”
693 of global environmental change. Proc. Nat. Acad. Sci. 106, 8085-8092.
694 Bonifacio, P., Bourgeois, S., Labrune, C., Amourous, J.M., Escoubeyrou, K., Buscail, R.,
695 Romero-Ramirez, A., Lantoine, F., Vetion, G., Bichon, S., Desmalades, M., Riviere, B.,
696 Deflandre, B., Gremare, A., 2014. Spatiotemporal changes in surface sediment
697 characteristics and benthic macrofauna composition off the Rhône River in relation to
698 its hydrological regime. Estuar. Coast. Shelf Sci. 151, 196-209.
699 Bourgeois, S., Pruski, A.M., Sun, M.Y., Buscail, R., Lantoine, F., Kerherve, P., Vetion, G.,
700 Riviere, B., Charles, F., 2011. Distribution and lability of land-derived organic matter
701 in the surface sediments of the Rhône prodelta and the adjacent shelf (Mediterranean
702 Sea, France): a multi proxy study. Biogeosciences 8, 3107-3125.
703 Cai, W.J., 2011. Estuarine and coastal ocean carbon paradox: CO_2 sinks or sites of
704 terrestrial carbon incineration. Ann. Rev. Mar. Sci. 3, 123-145.
705 Calmet, D., Fernandez, J.M., 1990. Caesium distribution in northwest Mediterranean
706 seawater, suspended particles and sediments. Cont. Shelf Res. 10, 895-913.
707 Cathalot, C., Rabouille, C., Pastor, L., Deflandre, B., Viollier, E., Buscail, R., Gremare, A.,
708 Treignier, C., Pruski, A., 2010. Temporal variability of carbon recycling in coastal
709 sediments influenced by rivers: assessing the impact of flood inputs in the Rhône River
710 prodelta. Biogeosciences 7, 1187-1205.

711 Cathalot, C., Rabouille, C., Tisnerat-Laborde, N., Toussaint, F., Kerherve, P., Buscail, R.,
712 Loftis, K., Sun, M.Y., Tronczynski, J., Azoury, S., Lansard, B., Treignier, C., Pastor, L.,
713 Tesi, T., 2013. The fate of river organic carbon in coastal areas: a study in the Rhône
714 River delta using multiple isotopic ($\delta^{13}C$, $\Delta^{14}C$) and organic tracers. Geochim.
715 Cosmochim. Acta 118, 33-55.
716 Cazala, C., Reyss, J.L., Decossas, J.L., Royer, A., 2003. Improvement in the
717 determination of ^{238}U, $^{228\text{-}234}Th$, $^{226\text{-}228}Ra$, ^{210}Pb and ^{7}Be by spectrometry on evaporated
718 fresh water samples. Environ.Sci. Technol. 37, 4990-4993.
719 Charmasson, S., 2003. ^{137}Cs inventory in sediment near the Rhône mouth: role played by
720 different sources. Oceanol. Acta 26, 435-441.
721 Charmasson, S., Bouisset, P., Radakovitch, O., Pruchon, A.S., Amaud, M., 1998.
722 Long-core profiles of ^{137}Cs, ^{134}Cs, ^{60}Co and ^{210}Pb in sediment near the Rhône River
723 (Northwestern Mediterranean Sea). Estuaries 21, 367-378.
724 Chen, C.T.A., Borges, A.V., 2009. Continental shelves as sinks and near-shore
725 ecosystems as sources of atmospheric CO_2. Deep-Sea Res. 56, 578-590.
726 Corbett, D.R., Dail, M., McKee, B., 2007. High-frequency time-series of the dynamic
727 sedimentation processes on the western shelf of the Mississippi River deltaic. Cont.
728 Shelf Res. 27, 1600-1615.
729 Corbett, D.R., McKee, B., Duncan, D., 2004. An evaluation of mobile mud dynamics in
730 the Mississippi River deltaic region. Mar. Geol. 209, 91-112.
731 Cutshall, N.H., Larsen, I.L., Olsen, C.R., 1983. Direct analysis of ^{210}Pb in sediment
732 samples: self-adsorption corrections. Nucl. Instrum. Methods 206, 309-312.
733 Dagg, M., Benner, R., Lohrenz, S., Lawrence, D., 2004. Transformation of dissolved and
734 particulate materials on continental shelves influenced by large rivers: plume processes.
735 Cont. Shelf Res. 24, 833-858.
736 De Madron, X.D., Abassi, A., Heussner, S., Monaco, A., Aloisi, J.C., Radakovitch, O.,
737 Giresse, P., Buscail, R., Kerherve, P., 2000. Particulate matter and organic carbon
738 budgets for the Gulf of Lions (NW Mediterranean). Oceanol. Acta 23, 717-730.
739 De Vismes Ott, A., Gurriaran, R., Cagnat, X., Masson, O., 2013. Fission product activity
740 ratios measured at trace level over France during the Fukushima accident. J. Environ.
741 Radioact. 125, 6-16.

742 Delanghe, D., Bard, E., Hamelin, B., 2002. New TIMS constraints on the uranium-238
743 and uranium-234 in seawaters from the main ocean basins and the Mediterranean Sea.
744 Mar. Chem. 80, 79-93.
745 Dibb, J.E., Rice, D.L., 1989. The geochemistry of beryllium-7 in Chesapeake Bay. Estuar.
746 Coast. Shelf Sci. 28, 379-394.
747 Drexler, T.M., Nittrouer, C.A., 2008. Stratigraphic signatures due to flood deposition near
748 the Rhône River: Gulf of Lions, northwest Mediterranean Sea. Cont. Shelf Res. 28,
749 1877-1894.
750 Dufois, F., Garreau, P., Le Hir, P., Forget, P., 2008. Wave- and current-induced bottom
751 shear stress distribution in the Gulf of Lions. Cont. Shelf Res. 28, 1920-1934.
752 Dufois, F., Verney, R., Le Hir, P., Dumas, F., Charmasson, S., 2014. Impact of winter
753 storms on sediment erosion in the Rhône River prodelta and fate of sediment in the
754 Gulf of Lions (North Western Mediterranean Sea). Cont. Shelf Res. 72, 57-72.
755 Durrieu de Madron, X., Abassi, A., Heussner, S., Monaco, A., Aloisi, J.C., Radakovitch,
756 O., Giresse, P., Buscail, R., Kerherve, P., 2000. Particulate matter and organic carbon
757 budgets for the Gulf of Lions (NW Mediterranean). Oceanol. Acta 23, 717-730.
758 Eyrolle, F., Charmasson, S., Louvat, D., 2004. Plutonium isotopes in the lower reaches of
759 the river Rhône over the period 1945-2000: fluxes towards the Mediterranean Sea and
760 sedimentary inventories. J. Environ. Radioact. 74, 127-138.
761 Eyrolle, F., Radakovitch, O., Raimbault, P., Charmasson, S., Antonelli, C., Ferrand, E.,
762 Aubert, D., Raccasi, G., Jacquet, S., Gurriaran, R., 2012. Consequences of
763 hydrological events on the delivery of suspended sediment and associated
764 radionuclides from the Rhône River to the Mediterranean Sea. J. Soils Sediment 12,
765 1479-1495.
766 Fanget, A.S., Bassetti, M.A., Arnaud, M., Chiffoleau, J.F., Cossa, D., Goineau, A.,
767 Fontanier, C., Buscail, R., Jouet, G., Maillet, G. M., Negri, A., Dennielou, B., Berne, S.,
768 2013. Historical evolution and extreme climate events during the last 400 years on the
769 Rhône prodelta (NW Mediterranean). Mar. Geol. 346, 375-391.
770 Fay, M.P., Proschan, M.A., 2010. Wilcoxon-Mann-Whitney or t-test? On assumptions for
771 hypothesis tests and multiple interpretations of decision rules. Stat. Surv. 4, 1-39.
772 Feng, H., Cochran, J. K., Hirschberg, D.J., 1999a. ^{234}Th and ^{7}Be as tracers for transport

and dynamics of suspended particles in a partially mixed estuary. Geochim. Cosmochim. Acta 63, 2487-2505.

Feng, H., Cochran, J.K., Hirschberg, D.J., 1999b. ^{234}Th and ^{7}Be as tracers for transport and sources of particle-associated contaminants in the Hudson River Estuary. Sci. Total Environ. 237/238, 401-418.

Ferrand, E., Eyrolle, F., Radakovitch, O., Provansal, M., Dufour, S., Vella, C., Raccasi, G., Gurriaran, R., 2012. Historical levels of heavy metals and artificial radionuclides reconstructed from overbank sediment records in lower Rhône River (South-East France). Geochim. Cosmochim. Acta 82, 163-182.

Fitzgerald, S.A., Klump, J.V., Swarzenski, P.W., Mackenzie, R.A., Richards, K.D., 2001. Beryllium-7 as a tracer of short-term sediment deposition and resuspension in the Fox River, Wisconsin. Environ. Sci. Technol. 35, 300-305.

Got, H., Aloisi, J.C., 1990. The Holocene sedimentation on the Gulf of Lions margin: a quantitative approach. Cont. Shelf Res. 10, 841-855.

Guo, L.D, Santschi, P.H., Baskaran, H., Zindler, A., 1995. Distribution of dissolved and particulate ^{230}Th and ^{232}Th in seawater from the Gulf of Mexico and off Cape Hatteras as measured by SIMS. Earth Planet. Sci. Lett. 133, 117-128.

IAEA, 2004. Sediment distribution coefficients and concentration factors for biota in the marine environment. Technical Reports Series 422, IAEA, Vienna, pp 95.

Ibanez, C., Pont, D., Prat, N., 1997. Characterization of the Ebre and Rhône estuaries: a basis for defining and classifying salt-wedge estuaries. Limnol. Oceanogr. 42, 89-101.

Ku, T.L., Knauss, K.G., Mathieu, G.G., 1977. Uranium in open ocean: concentration and isotopic composition. Deep-Sea Res. 24, 1005-1017.

Lal, D., Malhotra, P.K., Peters, B., 1958. On the production of radioisotopes in the atmosphere by cosmic radiation and their application to meteorology. J. Atoms. Terr. Phys. 12, 306-328.

Lansard, B., Charmasson, S., Gasco, C., Anton, M.P., Grenz, C., Arnaud, M., 2007. Spatial and temporal variations of plutonium isotopes (^{238}Pu and ^{239,240}Pu) in sediments off the Rhône River mouth (NW Mediterranean). Sci. Total Environ. 376, 215-227.

Lansard, B., Rabouille, C., Denis, L., Grenz, C., 2009. Benthic remineralization at the land-ocean interface: a case study of the Rhône River (NW Mediterranean Sea). Estuar.

804 Coast. Shelf Sci. 81, 544-554.
805 Larsen, I.L., Cutshall, N.H., 1981. Direct determination of ^{7}Be in sediments. Earth Planet.
806 Sci. Lett. 54, 379-384.
807 Lefevre, O., Bouisset, P., Germain, P., Barker, E., Kerlau, G., Cagnat, X., 2003.
808 Self-absorption correction factor applied to ^{129}I measurement by direct gamma-X
809 spectrometry for Fucus serratus samples. Nucl. Instr. Meth. Phys. Res. A 506, 173-185.
810 Maillet, G.M., Vella, C., Berne, S., Friend, P.L., Amos, C.L., Fleury, T.J., Normand, A.,
811 2006. Morphological changes and sedimentary processes induced by the December
812 2003 flood event at the present mouth of the Grand Rhône River (southern France).
813 Mar. Geol. 234, 159-177.
814 Mangini, A., Sonntag, C., Bertsch, G., Muller, E., 1979. Evidence for a high natural
815 uranium content in world rivers. Nature 278, 337-339.
816 Many, G., Bourrin, F., Durrieu de Madron, X., Pairaud, I., Gangloff, A., Doxaran, D., Ody,
817 A., Verney, R., Menniti, C., Le Berre, D., Jacquet, M., 2016. Particle assemblage
818 characterization in the Rhône River ROFI. J. Mar. Syst. 157, 39-51.
819 Many, G., Bourrin, F., Durrieu de Madron, X., Ody, A., Doxaran, D., 2018. Glider and
820 satellite monitoring of the variability of the suspended particle distribution and size in
821 the Rhône ROFI. Progr. Oceano, 163, 123-135.
822 Marion, C., Dufois, F., Arnaud, M., Vella, C., 2010. In situ record of sedimentary
823 processes near the Rhône River mouth during winter events (Gulf of Lions,
824 Mediterranean Sea). Cont. Shelf Res. 30, 1095-1107.
825 Matisoff, G., Bonniwell, E.C., Whiting, P.J., 2002. Soil erosion and sediment sources in
826 an Ohio watershed using beryllium-7, cesium-137, and lead-210. J. Environ. Qual. 31,
827 54-61.
828 McCubbin, D., Leonard, K.S., Greenwood, R.C., Taylor, B.R., 2004. Solid-solution
829 partitioning of plutonium in surface waters at the Atomic Weapons Establishment
830 Aldermaston (UK). Sci. Total Environ. 332, 203-216.
831 McKee, B.A., Aller, R.C., Allison, M.A., Bianchi, T.S., Kineke, G.C., 2004. Transport
832 and transformation of dissolved and particulate materials on continental margins
833 influenced by major rivers: benthic boundary layer and seabed processes. Cont. Shelf
834 Res. 24, 899-926.

Milliams, J., Rose, C.P., 2001. Measured and predicted rates of sediment transport in storm conditions. Mar. Geol. 179, 121-133.

Miralles, J., Arnaud, M., Radakovitch, O., Marion, C., Cagnat, X., 2006. Radionuclide deposition in the Rhône River Prodelta (NW Mediterranean Sea) in response to the December 2003 extreme flood. Mar. Geol. 234, 179-189.

Miralles, J., Radakovitch, O., Aloisi, J.C., 2005. ^{210}Pb sedimentation rates from the Northwestern Mediterranean margin. Mar. Geol. 216, 155-167.

Miralles, J., Radakovitch, O., Cochran, J.K., Veron, A., Masque, P., 2004. Multitracer study of anthropogenic contamination records in the Camargue, Southern France. Sci. Total Environ. 320, 63-72.

Moore, W.S., de Oliveira, J., 2008. Determination of residence time and mixing processes of the Ubatuba, Brazil, inner shelf waters using natural Ra isotopes. Estuar. Coast. Shelf Sci. 76, 512-521.

Mullenbach, B.L., Nittrouer, C.A., Puig, P., Orange, D.L., 2004. Sediment deposition in a modern submarine canyon: Eel Canyon, Northern California. Mar. Geol. 211, 101-119.

Naudin, J.J., Cauwet, G., Chretiennot-Dinet, M.J., Deniaux, B., Devenon, J.L., Pauc, H., 1997. River discharge and wind influence upon particulate transfer at the land-ocean interaction: case study of the Rhône River plume. Estuar. Coast. Shelf Sci. 45, 303-316.

Ogston, A.S., Drexler, T.M., Puig, P., 2008. Sediment delivery, resuspension, and transport in two contrasting canyon environments in the southwest Gulf of Lions. Cont. Shelf Res. 28, 2000-2016.

Ollivier, P., Radakovitch, O., Hamelin, B., 2011. Major and trace element partition and fluxes in the Rhône River. Chem. Geol. 285, 15-31.

Olsen, C.R., Larsen, I.L., Lowry, P.D., Cutshall, N.H., Nichols, M.M., 1986. Geochemistry and deposition of ^{7}Be in river-estuarine and coastal water. J. Geophys. Res. 91, 896-908.

Owens, S.A., Buesseler, K.O., Sims, K.W.W., 2012. Re-evaluating the ^{238}U-salinity relationship in seawater: implications for the ^{238}U-^{234}Th disequilibrium method. Mar. Chem. 127, 31-39.

Palinkas, C.M., Nittrouer, C.A., Wheatcroft, R.A., Langone, L., 2005. The use of ^{7}Be to

identify event and seasonal sedimentation near the Po River delta, Adriatic Sea. Mar. Geol. 222/223, 95-112.

Pastor, L., Deflandre, B., Viollier, E., Cathalot, C., Metzger, E., Rabouille, C., Escoubeyrou, K., Lloret, E., Pruski, A.M., Vetion, G., Desmalades, M., Buscail, R., Gremare, A., 2011. Influence of the organic matter composition on benthic oxygen demand in the Rhône River prodelta (NW Mediterranean Sea). Cont. Shelf Res. 31, 1008-1019.

Perianez, R., 2005. Modelling the transport of suspended particulate matter by the Rhône River plume (France). Implications for pollutant dispersion. Environ. Pollut. 133, 351-364.

Pont, D., Simonnet, J.P., Walter, A.V., 2002. Medium-term changes in suspended sediment delivery to the ocean: consequences of catchment heterogeneity and river management (Rhône River, France). Estuar. Coast. Shelf Sci. 54, 1-18.

Radakovitch, O., Charmasson, S., Arnaud, M., Bouisset, P., 1999. ^{210}Pb and caesium accumulation in the Rhône delta sediment. Estuar. Coast. Shelf Sci. 48, 77-99.

Radakovitch, O., Roussiez, V., Ollivier, P., Ludwig, W., Grenz, C., Probst, J.L., 2008. Input of particulate heavy metals from rivers and associated sedimentary deposits on the Gulf of Lion continental shelf. Estuar. Coast. Shelf Sci. 77, 285-295.

Rassmann, J., Lansard, B., Pozzato, L., Rabouille, C., 2016. Carbonate chemistry in sediment porewaters of the Rhône River delta driven by early diagenesis (northwestern Mediterranean). Biogeosciences 13, 5379-5394.

Reyss, J.L., Schmidt, S., Legeleux, F., Bonté, P., 1995. Large, low background well type detectors for the measurement of environmental radioactivity. Nucl. Instrum. Methods Physic. Res. Sec A 357, 391-397.

Roussiez, V., Aloisi, J.C., Monaco, A., Ludwig, W., 2005. Early muddy deposits along the Gulf of Lions shoreline: A key for a better understanding of land-to-sea transfer of sediments and associated pollutant fluxes. Mar. Geol. 222-223, 345-358.

Roussiez, V., Ludwig, W., Monaco, A., Probst, J.L., Bouloubassi, I., Buscail, R., Saragoni, G., 2006. Sources and sinks of sediment-bound contaminants in the Gulf of Lions (NW Mediterranean Sea): a multi-tracer approach. Cont. Shelf Res. 26, 1843-1857.

Saari, H.K., Schmidt, S., Castaing, P., Blanc, G., Sautour, B., Masson, O., Cochran, J.K.,

2010. The particulate $^{7}Be/^{210}Pb_{xs}$ and $^{234}Th/^{210}Pb_{xs}$ activity ratios as tracers for tidal-to-seasonal particle dynamics in the Gironde estuary (France): Implications for the budget of particle-associated contaminants. Sci. Total Environ. 408, 4784-4794.

Sadaoui, M., Ludwig, W., Bourrin, F., Raimbault, P., 2016. Controls, budgets and variability of riverine sediment fluxes to the Gulf of Lions (NW Mediterranean Sea). J. Hydrol. 540, 1002-1015.

Sanford, L.P., 1992. New sedimentation, resuspension, and burial. Limnol. Oceanogr. 37, 1164-1178.

Santschi, P.H., Guo, L., Walsh, I.D., Quigley, M.S., Baskaran, M., 1999. Boundary exchange and scavenging of radionuclides in continental margin waters of the Middle Atlantic Bight: implications for organic carbon fluxes. Cont. Shelf Res. 19, 609-636.

Sempéré, R., Charriere, B., Van Wambeke, F., Cauwet, G., 2000. Carbon inputs of the Rhône River to the Mediterranean Sea: biogeochemical implications. Glob. Biogeochem. Cy. 14, 669-681.

Skwarzec, B., 1995. Polonium, uranium and plutonium in southern Baltic ecosystem. Thesis and monographies, Institute of Oceanology PAN, 6, Sopot.

Sommerfield, C.K., Nittrouer, C.A., Alexander, C.R., 1999. ^{7}Be as a tracer of flood sedimentation on the northern California continental margin. Cont. Shelf Res. 19, 335-361.

Su, N., Du, J., Moore, W.S., Liu, S., Zhang, J., 2011. An examination of groundwater discharge and the associated nutrient fluxes into the estuaries of eastern Hainan Island, China using ^{226}Ra. Sci. Total Environ. 409, 3909-3918.

Syvitski, J.P.M., Saito, Y., 2007. Morphodynamics of deltas under the influence of humans. Glob. Planet. Change 57, 261-282.

Taylor, A., Blake, W.H., Smith, H.G., Mabit, L., Keith-Roach, M.J., 2013. Assumptions and challenges in the use of fallout beryllium-7 as a soil and sediment tracer in river basins. Earth Sci. Rev. 126, 85-95.

Thill, A., Moustier, S., Garnier, J.M., Estournel, C., Naudin, J.J., Bottero, J.Y., 2001. Evolution of particle size and concentration in the Rhône River mixing zone: influence of salt flocculation. Cont. Shelf Res. 21, 2127-2140.

Ulses, C., Estournel, C., Durrieu de Madron, X., Palanques, A., 2008. Suspended

928 sediment transport in the Gulf of Lions (NW Mediterranean): impact of extreme storms
929 and floods. Cont. Shelf Res. 28, 2048-2070.
930 Wallbrink, P.J., Murray, A.S., 1994. Fallout of ^{7}Be in south Eastern Australia. J. Environ.
931 Radioact. 25, 213-228.
932 Wallbrink, P.J., Murray, A.S., 1996. Distribution and variability of ^{7}Be in soils under
933 different surface cover conditions and its potential for describing soil redistribution
934 processes. Water Resour. Res. 32, 467-476.
935 Wang, J.L., Du, J.Z., Baskaran, M., Zhang, J., 2016. Mobile mud dynamics in the East
936 China Sea elucidated using ^{210}Pb, ^{137}Cs, ^{7}Be, and ^{234}Th as tracers. J. Geophys. Res.
937 Oceans 121, 224-239.
938 Wang, Z.L., Yamada, M., 2005. Plutonium activities and ^{240}Pu/^{239}Pu atom ratios in
939 sediment cores from the East China Sea and Okinawa Trough: sources and inventories.
940 Earth Planet. Sci. Lett. 233, 441-453.
941 Yeager, K.M., Santschi, P.H., Rowe, G.T., 2004. Sediment accumulation and radionuclide
942 inventories (Pu-239, Pu-240, Pu-210 and Th-234) in the northern Gulf of Mexico, as
943 influenced by organic matter and macrofaunal density. Mar. Chem. 91, 1-14.
944 Zebracki, M., Cagnat, X., Gairoard, S., Cariou, N., Eyrolle, F., Boulet, B., Antonelli, C.,
945 2017. U isotopes distribution in the lower Rhône River and its implication on
946 radionuclides disequilibrium within the decay series. J. Environ. Radioact. 178-179,
947 279-289.
948 Zebracki, M., Eyrolle, F., Evrard, O., Claval, D., Mourier, B., Gairoard, S., Cagnat, X.,
949 Antonelli, C., 2015. Tracing the origin of suspended sediment in a large Mediterranean
950 river by combining continuous river monitoring and measurement of artificial and
951 natural radionuclides. Sci. Total Environ. 502, 122-132.